Ocean acidification of a coastal Antarctic marine microbial community reveals a critical threshold for CO_2 tolerance in phytoplankton productivity

Stacy Deppeler[1], Katherina Petrou[2], Kai G. Schulz[3], Karen Westwood[4,5], Imojen Pearce[4], John McKinlay[4], and Andrew Davidson[4,5]

[1]Institute for Marine and Antarctic Studies, University of Tasmania, Private Bag 129, Hobart, Tasmania 7001, Australia
[2]School of Life Sciences, University of Technology Sydney, 15 Broadway, Ultimo, New South Wales 2007, Australia
[3]Centre for Coastal Biogeochemistry, Southern Cross University, Military Rd, East Lismore, NSW, 2480, Australia
[4]Australian Antarctic Division, Department of the Environment and Energy, 203 Channel Highway, Kingston, Tasmania 7050, Australia
[5]Antarctic Climate and Ecosystems Cooperative Research Centre, Private Bag 80, Hobart, Tasmania 7001, Australia

Correspondence to: Stacy Deppeler (stacy.deppeler@utas.edu.au)

Abstract.

High-latitude oceans are anticipated to be some of the first regions affected by ocean acidification. Despite this, the effect of ocean acidification on natural communities of Antarctic marine microbes is still not well understood. In this study we exposed an early spring, coastal marine microbial community in Prydz Bay to CO_2 levels ranging from ambient (343 μatm) to 1641

5 μatm in six 650 l minicosms. Productivity assays were performed to identify whether a CO_2 threshold existed that led to a change in primary productivity, bacterial productivity, and the accumulation of Chlorophyll a (Chl a) and particulate organic matter (POM) in the minicosms. In addition, photophysiological measurements were performed to identify possible mechanisms driving changes in the phytoplankton community. A critical threshold for tolerance to ocean acidification was identified in the phytoplankton community between 953 and 1140 μatm. CO_2 levels $\geq$1140 μatm negatively affected photosynthetic

10 performance and Chl a-normalised primary productivity (csGPP$_{14C}$), causing significant reductions in gross primary production (GPP$_{14C}$), Chl a accumulation, nutrient uptake, and POM production. However, there was no effect of CO_2 on C:N ratios. Over time, the phytoplankton community acclimated to high CO_2 conditions, showing a down-regulation of carbon concentrating mechanisms (CCMs) and likely adjusting other intracellular processes. Bacterial abundance initially increased in CO_2 treatments $\geq$953 μatm (days 3-5), yet gross bacterial production (GBP$_{14C}$) remained unchanged and cell-specific bacterial

15 productivity (csBP$_{14C}$) was reduced. Towards the end of the experiment, GBP$_{14C}$ and csBP$_{14C}$ markedly increased across all treatments regardless of CO_2 availability. This coincided with increased organic matter availability (POC and PON) combined with improved efficiency of carbon uptake. Changes in phytoplankton community production could have negative effects on the Antarctic food web and the biological pump, resulting in negative feedbacks on anthropogenic CO_2 uptake. Increases in bacterial abundance under high CO_2 conditions may also increase the efficiency of the microbial loop, resulting in increased

20 organic matter remineralisation and further declines in carbon sequestration.

1 Introduction

The Southern Ocean (SO) is a significant sink for anthropogenic CO_2 (Metzl et al., 1999; Sabine et al., 2004; Frölicher et al., 2015). Approximately 30% of anthropogenic CO_2 emissions have been absorbed by the world's oceans, of which 40% has been

5 via the SO (Raven and Falkowski, 1999; Sabine et al., 2004; Khatiwala et al., 2009; Takahashi et al., 2009, 2012; Frölicher et al., 2015). While ameliorating CO_2 accumulation in the atmosphere, increasing oceanic CO_2 uptake alters the chemical balance of surface waters, with the average pH having already decreased by 0.1 units since pre-industrial times (Sabine et al., 2004; Raven et al., 2005). If anthropogenic emissions continue unabated, future concentrations of CO_2 in the atmosphere are projected to reach $\sim$930 µatm by 2100 and peak at $\sim$2000 µatm by 2250 (Meinshausen et al., 2011; IPCC, 2013). This will

10 result in a further reduction of the surface ocean pH by up to 0.6 pH units, with unknown consequences to the marine microbial community (Caldeira and Wickett, 2003). High-latitude oceans have been identified as amongst the first regions to experience the negative effects of ocean acidification, causing potentially harmful reductions in the aragonite saturation state and a decline in the ocean's capacity for future CO_2 (Sabine et al., 2004; Orr et al., 2005; McNeil and Matear, 2008; Fabry et al., 2009; Hauck and Völker, 2015). Marine microbes play a pivotal role in the uptake and storage of CO_2 in the ocean, through phytoplankton

15 photosynthesis and vertical transport of biological carbon to the deep ocean (Longhurst, 1991; Honjo, 2004). As the buffering capacity of the SO decreases over time, the biological contribution to total CO_2 uptake is expected to increase in importance (Hauck et al., 2015; Hauck and Völker, 2015). Thus, it is necessary to understand the effects of high CO_2 on the productivity of the marine microbial community if we are to predict how they may affect ocean biogeochemistry in the future.

Phytoplankton primary production provides the food source to higher trophic levels and plays a critical role in the seques-

20 tration of carbon from the atmosphere into the deep ocean (Azam et al., 1983, 1991; Longhurst, 1991; Honjo, 2004; Fenchel, 2008; Kirchman, 2008). In Antarctic waters it is restricted to a short summer season and is characterised by intense phytoplankton blooms that can reach over $200 \, \mathrm{mg} \, \mathrm{Chl} \, a \, \mathrm{m}^{-2}$ (Smith and Nelson, 1986; Nelson et al., 1987; Wright et al., 2010). Relative to elsewhere in the SO, the continental shelf around Antarctica accounts for a disproportionately high percentage of annual primary productivity (Arrigo et al., 2008a). In coastal Antarctic waters, seasonal CO_2 variability can be up to 450 µatm

25 over a year (Gibson and Trull, 1999; Boyd et al., 2008; Moreau et al., 2012; Roden et al., 2013; Tortell et al., 2014). Sea ice forms a barrier to outgassing of CO_2 in winter, causing supersaturation of the surface water to $\sim$500 µatm. Intense primary productivity in summer rapidly draws down CO_2 to $<$100 µatm, making this region a significant CO_2 sink during summer months (Hoppema et al., 1995; Ducklow et al., 2007; Arrigo et al., 2008b).

Ocean acidification studies on individual phytoplankton species have reported differing trends in primary productivity and

30 growth rates. Increased CO_2 enhanced rates of primary productivity (Wu et al., 2010; Trimborn et al., 2013) and growth (Sobrino et al., 2008; Tew et al., 2014; Baragi et al., 2015; Chen et al., 2015; King et al., 2015) in some diatom species, while others have been shown to remain unaffected (Chen and Durbin, 1994; Sobrino et al., 2008; Berge et al., 2010; Trimborn et al., 2013; Chen et al., 2015; Hoppe et al., 2015; King et al., 2015; Bi et al., 2017). In contrast, CO_2-related declines in

primary productivity and growth rate have also been observed (Barcelos e Ramos et al., 2014; Hoppe et al., 2015; King et al., 2015; Shi et al., 2017), suggesting that responses to ocean acidification are largely species-specific. These differing responses among phytoplankton species may also cause changes in the composition of phytoplankton communities (Trimborn et al., 2013). It is difficult to extrapolate the response of individual species to natural communities, as monospecific studies exclude interactions among species and trophic levels. Estimates of CO_2 tolerance under laboratory conditions may also be influenced by experimental acclimation periods (Trimborn et al., 2014; Hennon et al., 2015; Torstensson et al., 2015; Li et al., 2017a), differences in experimental conditions (e.g. nutrients, light climate) (Hoppe et al., 2015; Hong et al., 2017; Li et al., 2017b), methods of CO_2 manipulation (Shi et al., 2009; Gattuso et al., 2010), as well as region-specific environmental adaptations (Schaum et al., 2012). Thus, investigations on natural communities are essential in order to better understand the outcome of these complex interactions.

The effects of ocean acidification on natural Antarctic phytoplankton communities is currently not well understood (Petrou et al., 2016; Deppeler and Davidson, 2017). Tolerance to CO_2 levels up to $\sim$800 µatm have been reported for natural coastal communities in the West Antarctic Peninsula and Prydz Bay, East Antarctica (Young et al., 2015; Davidson et al., 2016). Although in Prydz Bay, when CO_2 levels exceeded 780 µatm, primary productivity declined and community composition shifted toward smaller, picoeukaryotes (Davidson et al., 2016; Thomson et al., 2016; Westwood et al., submitted). In contrast, Ross Sea phytoplankton communities responded to CO_2 levels $\geq$750 µatm with an increase in primary productivity and abundance of large chain-forming diatoms, suggesting that as CO_2 increases in this region, diatoms may increase in dominance over the prymnesiophyte *Phaeocystis antarctica* (Tortell et al., 2008b; Feng et al., 2010). The paucity of information regarding the ocean acidification response of these Antarctic coastal phytoplankton communities highlights the need for further research to determine region-specific tolerances and potential tipping points in community productivity and composition in Antarctica.

Bacteria play an essential role in the microbial food web through the remineralisation of nutrients from sinking particles (Azam et al., 1991) and as a food source for heterotrophic nanoflagellates (Pearce et al., 2010). Bacterial populations respond to increases in phytoplankton primary productivity by increasing their productivity and abundance, with maximum abundance often occurring after the peak of the phytoplankton bloom (Pearce et al., 2007). High CO_2 levels have been observed to have either no effect on abundance and productivity (Grossart et al., 2006; Allgaier et al., 2008; Paulino et al., 2008; Baragi et al., 2015; Wang et al., 2016) or increase growth rate and production only during the post-bloom phase of an experiment (Grossart et al., 2006; Sperling et al., 2013; Westwood et al., submitted). Thus, bacterial communities appear to be relatively tolerant to ocean acidification, with bacterial growth indirectly affected by ocean acidification responses of the phytoplankton community (Grossart et al., 2006; Allgaier et al., 2008; Engel et al., 2013; Piontek et al., 2013; Sperling et al., 2013; Bergen et al., 2016).

Mesocosm experiments are an effective way of monitoring the community response of microbial assemblages to environmental changes. Experiments examining multiple species and trophic levels can provide responses that differ significantly from mono-specific studies. Numerous mesocosm studies have now been performed, assessing the effect of ocean acidification on natural marine microbial communities around the world (e.g. Kim et al., 2006; Hopkinson et al., 2010; Riebesell et al., 2013; Paul et al., 2015; Bach et al., 2016; Bunse et al., 2016). Studies in the Arctic reported increases in phytoplankton primary productivity, growth, and organic matter concentration at CO_2 levels $\geq$800 µatm under nutrient-replete conditions (Bellerby

et al., 2008; Egge et al., 2009; Engel et al., 2013; Schulz et al., 2013), whilst the bacterial community was unaffected (Grossart et al., 2006; Allgaier et al., 2008; Paulino et al., 2008; Baragi et al., 2015). These studies also highlight the importance of nutrient availability on the community response to elevated CO_2, with substantial differences in primary and bacterial productivity, Chlorophyll a (Chl a), and elemental stoichiometry observed between nutrient-replete and nutrient-limited conditions (Riebesell et al., 2013; Schulz et al., 2013; Sperling et al., 2013; Bach et al., 2016).

Previous community-level studies investigating the effects of ocean acidification on natural coastal marine microbial communities in East Antarctica reported declines in primary and bacterial productivity when CO_2 levels exceeded 780 µatm (Westwood et al., submitted). To build upon the results of Westwood et al. (submitted), a similar experimental design was utilised, with a natural marine microbial community from the same region exposed to CO_2 levels ranging from 343 to 1641 µatm in 650 l minicosms. The methods were refined in our study to include an acclimation period to the CO_2 treatment under low light. Rates of primary productivity, bacterial productivity, and the accumulation of particulate organic matter (POM) were examined to ascertain whether the threshold for tolerance to CO_2 was similar to that reported by Westwood et al. (submitted), or if acclimation affected the community response to high CO_2. Photophysiological measurements were also undertaken to assess underlying mechanisms that caused shifts in phytoplankton community productivity.

2 Methods

2.1 Minicosm setup

Natural microbial assemblages were incubated in six 650 l polythene tanks (minicosms) housed in a temperature controlled shipping container (Fig. 1). All minicosms were acid washed with 10% vol:vol AR HCl, thoroughly rinsed with MilliQ water, and given a final rinse with seawater from the sampling site before use. The minicosms were filled with seawater taken amongst decomposing fast ice in Prydz Bay, at Davis Station, Antarctica (68° 35' S 77° 58' E) on 19th November 2014. Water was transferred by helicopter in multiple collections using a 720 l Bambi Bucket to fill a 7000 l polypropylene holding tank. Seawater was gravity fed into the minicosm tanks through Teflon lined hosing fitted with an in-line 200 µm Arkal filter to exclude metazooplankton. All minicosms were filled simultaneously to ensure uniform distribution of microbes in all tanks.

The ambient water temperature at the time of sampling in Prydz Bay was -1.0 °C. Tanks were temperature controlled to an average temperature of 0.0 °C, with a maximum range of ± 0.5 °C, through cooling of the shipping container and warming with two 300W aquarium heaters (Fluval) that were connected to a temperature control program via Carel temperature controllers. The contents of each tank were gently mixed by a shielded high density polyethylene auger, rotating at 15 rpm, and each tank was covered with a sealed acrylic lid.

Each tank was illuminated on a 19:5 hr light:dark cycle by two 150W HQI-TS/NDL (Osram) metal halide lamps (transmission spectra: www.osram.com.au/media/resource/hires/335357/powerstar-hqi-ts-excellence-70-w-and-150-w—the-latest-innovation-in-quartz-tec.pdf). The light output was filtered by a light-scattering filter and a one quarter colour temperature (CT) blue filter (Arri) to convert the tungsten lighting to a daylight spectral distribution, attenuating wavelengths <500 nm by ~20% and >550 nm by ~40% (Davidson et al., 2016).

Similar to Schulz et al. (2017) the fugacity of carbon dioxide ($f\mathrm{CO_2}$) in each tank was raised to the target concentration in a step-wise manner over the first 5 days of the incubation (Fig. 2, see below). During this acclimation, phytoplankton growth in the tanks was slowed by attenuating the light intensity to 0.9 ± 0.2 µmol photons $\mathrm{m^{-2}\,s^{-1}}$ using two 90% neutral density (ND) filters (Arri).

At the conclusion of this CO2 acclimation period, the light intensity was increased for 24 hrs through replacement of the two 90% ND filters with one 60% ND filter. The final light intensity was achieved on day 7 with a one quarter CT blue and a light-scattering filter, which proved to be saturating for photosynthesis (see below).

Unless otherwise specified, samples were taken for analyses on days 1, 3, and 5 during the $\mathrm{CO_2}$ acclimation period and every 2 days from day 8 to 18.

2.2 Carbonate chemistry measurements and calculations

Samples for carbonate chemistry measurements were collected daily from each minicosm in 500 ml glass stoppered bottles (Schott Duran) following the guidelines of Dickson et al. (2007). Sub-samples for dissolved inorganic carbon (DIC, 50 ml glass stoppered bottles) and pH on the total scale ($\mathrm{pH_T}$, 100 ml glass stoppered bottles) measurements were gently pressure filtered (0.2 µm) with a peristaltic pump at a flow rate of $\sim$30 ml min^{-1}, similar to Bockmon and Dickson (2014).

DIC was measured by infra-red absorption on an Apollo SciTech AS-C3 analyzer equipped with a LICOR LI-7000 detector using triplicate 1.5 ml samples. The instrument was calibrated (and checked for linearity) within the expected DIC concentration range with five sodium carbonate standards (Merck Suprapur) that were dried for 2 hours at 230 °C and prepared gravimetrically in milliQ water (18.2 MΩ cm^{-1}) at 25 °C. Furthermore, daily measurements of certified reference material batch CRM127 (Dickson, 2010) were used for improved accuracy. Volumetrically measured DIC was converted to µmol kg^{-1} using calculated density derived from known temperature and salinity. The typical precision among triplicate measurements was <2 µmol kg^{-1}.

$\mathrm{pH_T}$ was measured spectrophotometrically (GBC UV-Vis 916) in a ten centimetre thermostated (25 °C) cuvette using the pH indicator dye m-cresol purple (Acros Organics, 62625-31-4, Lot A0321770) following the approach described in Dickson et al. (2007), which included changes in sample pH due to dye addition. Contact with air was minimized by sample delivery, dye addition, and mixing via a syringe pump (Tecan, Cavro XLP6000). Dye impurities and instrument performance were accounted for by applying a constant off-set (+0.003 pH units), determined by the comparison of measured and calculated $\mathrm{pH_T}$ (from known DIC and total alkalinity (TA), including silicate and phosphate) of CRM127. Typical measurement precision for triplicates was 0.001 for higher and 0.003 for lower pH treatments. For further details see Schulz et al. (2017).

Carbonate chemistry speciation was calculated from measured DIC and $\mathrm{pH_T}$. In a first step, at in situ measured salinities (WTW197 conductivity meter), practical alkalinity (PA) was calculated at 25 °C using the dissociation constants for carbonic acid determined by Mehrbach et al. (1973) as refitted by Lueker et al. (2000). Then, total carbonate chemistry speciation was calculated from measured DIC and calculated PA for in situ temperature conditions.

2.3 Carbonate chemistry manipulation

The $f\text{CO}_2$ in the minicosms was adjusted by additions of 0.22 μm-filtered natural seawater that was saturated by bubbling with AR grade CO_2 for $\geq$30 mins. In order to keep $f\text{CO}_2$ as constant as possible throughout the experiment, pH in each minicosm was measured with a portable, NBS-calibrated probe (Mettler Toledo) in the morning before sampling and the afternoon, to estimate the necessary amount of DIC to be added. The required volume of CO_2 enriched seawater was then transferred into 1000 ml infusion bags and added to the individual minicosms at a rate of about 50 ml min^{-1}. After reaching target levels, the mean $f\text{CO}_2$ levels in the minicosms were 343, 506, 634, 953, 1140, and 1641 μatm (Table S1).

2.4 Light irradiance

Average light intensity in each minicosm tank was calculated by measuring light intensity in the empty tanks at three depths (top, middle, and near-bottom) and across each tank (left, middle, and right) using a Biospherical Instruments' Laboratory Quantum Scalar Irradiance Meter (QSL-101). The average light irradiance received by phytoplankton within each tank was calculated following the equation of Riley (1957) (Table 1). Incoming irradiance ($\bar{I}_o$) was calculated as the average light intensity across the top of the tank. The average vertical light attenuation (K_d) was calculated as the slope from regression of the natural log of light intensity at all three depths, and mixed depth (Z_m) was the depth of the minicosm tanks (1.14 m).

Changes in vertical light attenuation due to increases in Chl a concentration throughout the experimental period were calculated from the equation in Westwood et al. (submitted); $K_{d(biomass)} = 0.0451157 \times$ Chl a (mg m^{-3}). Total light attenuation $K_{d(total)}$ in each tank at each sampling day was calculated by addition of K_d and $K_{d(biomass)}$.

2.5 Nutrient analysis

No nutrients were added to the minicosms during the experiment. Macronutrient samples were obtained from each minicosm following the protocol of Davidson et al. (2016). Seawater was filtered through 0.45 μm Sartorius filters into 50 ml Falcon tubes and frozen at -20 °C for analysis in Australia. Concentrations of ammonia, nitrate plus nitrite (NOx), soluble reactive phosphorus (SRP), and molybdate reactive silica (Silica) were determined using flow injection analysis by Analytical Services Tasmania following Davidson et al. (2016).

2.6 Elemental analysis

Samples for POM analysis, particulate organic carbon (POC) and particulate organic nitrogen (PON), were collected following the method of Pearce et al. (2007). Equipment for sample preparation was soaked in Decon 20 (Decon Laboratories) for >2 days and thoroughly rinsed in MilliQ water before use. Forceps and cutting blades were rinsed in 100% acetone between samples. Seawater was filtered through muffled 25 mm Sartorius Quartz microfibre filters until clogged. The filters were folded in half and frozen at -20 °C for analysis in Australia. Filters were thawed and opposite one-eighth sub-samples were cut and transferred into a silver POC cup (Elemental Analysis Ltd). Inorganic carbon was removed from each sample through addition of 20 μl of 2N HCl to each cup and drying at 60 °C for 36 hrs. When dry, each cup was folded shut, compressed into a pellet,

and stored in desiccant until analysed at the Central Science Laboratory, University of Tasmania, using a Thermo Finnigan EA 1112 Series Flash Elemental Analyser.

2.7   Chlorophyll *a*

Seawater was collected from each minicosm and a measured volume was filtered through 13 mm Whatman GF/F filters (maximum filtration time of 20 min). Filters were folded in half, blotted dry, and immediately frozen in liquid nitrogen for analysis in Australia. Chlorophyll *a* (Chl *a*)Pigments were extracted, analysed by HPLC, and quantified following the methods of Wright et al. (2010). Chl *a* was extracted from filters with 300 µl dimethylformamide plus 50 µl methanol, containing 140 ng apo-8'-carotenal (Fluka) internal standard, followed by bead beating and centrifugation to separate the extract from particulate matter. Extracts (125 µl) were diluted to 80% with water and analysed on a Waters HPLC using a Waters Symmetry C8 column and a Waters 996 photodiode array detector. Chl *a* was identified by its retention time and absorption spectra compared to a mixed standard sample from known cultures (Jeffrey and Wright, 1997), run daily before samples. Peak integrations were performed using Waters Empower software, checked manually for corrections, and quantified using the internal standard method (Mantoura and Repeta, 1997).

2.8 ^{14}C primary productivity

Primary productivity incubations were performed following the method of Westwood et al. (2010), based on the technique of Lewis and Smith (1983). This method incubated phytoplankton for 1 hr, minimising respiratory losses of photo-assimilated ^{14}C so that the uptake nearly approximated gross primary productivity (e.g. Dring and Jewson, 1982; González et al., 2008; Regaudie-de gioux et al., 2014). Samples were analysed for total organic carbon (TO^{14}C) content, thereby including any ^{14}C-labelled photosynthate leaked to the dissolved organic carbon (DO^{14}C) pool (Regaudie-de gioux et al., 2014).

For all samples, 5.92 MBq (0.16 mCi) of ^{14}C-sodium bicarbonate (NaH^{14}CO$_3$, PerkinElmer) was added to 162 ml of seawater from each minicosm, creating a working solution of 37 kBq ml^{-1}. Aliquots of this working solution (7 ml) were then added to glass scintillation vials and incubated for 1 hr at 21 light intensities, ranging from 0 - 1412 µmol photons m^{-2} s^{-1}. The temperature within each of the vials was maintained at -1.0 ± 0.3 °C through water cooling of the incubation chamber. The reaction was terminated with the addition of 250 µl of 6N HCl and the vials were shaken for 3 hours at 200 rpm to remove dissolved inorganic carbon. Duplicate time zero (T$_0$) samples were set up in a similar manner to determine background radiation, with 250 µl of 6N HCl added immediately to quench the reaction without exposure to light. Duplicate 100% samples were also performed to determine the activity of the working solution for each tank. For each 100% sample, 100 µl of working solution was added to 7 ml 0.1M NaOH in filtered seawater to bind all ^{14}C. For radioactive counts, 10 ml Ultima Gold LLT scintillation cocktail (PerkinElmer) was added to each scintillation vial, shaken, and decays per minute (DPM) were counted in a PerkinElmer Tri-Carb 2910TR Low Activity Liquid Scintillation Analyzer with a maximum counting time set at 3 min.

DPM counts were converted into primary productivity following the equation of Steemann Nielsen (1952) (Table 1), using measured DIC concentrations (varying between ∼2075 - 2400 µmol kg^{-1}) and normalised to Chl *a* using minicosm Chl *a* concentration (see above). Photosynthesis versus irradiance (PE) curves were modelled for each treatment following the equation

7

of Platt et al. (1980) using the *Phytotools* package in R (Silsbe and Malkin, 2015; R Core Team, 2016). Photosynthetic parameter estimates included the light-saturated photosynthetic rate (P_{max}), maximum photosynthetic efficiency (α), photoinhibition rate (β), and saturating irradiance (E_k). Modelled Chl *a*-specific primary productivity (csGPP$_{14C}$) was calculated following the equation of Platt et al. (1980) using average minicosm light irradiance ($\bar{I}$). Gross primary production rates (GPP$_{14C}$) in each tank were calculated from modelled csGPP$_{14C}$ and Chl *a* concentration (see above). Calculations and units for each parameter are presented in Table 1.

2.9 Gross community productivity

Community photosynthesis and respiration rates were measured using custom-made mini-chambers. The system consisted of four, 5.1 ml glass vials with oxygen sensor spots (Pyroscience) attached on the inside of the vials using non-toxic silicon glue. The vials were sealed, ensuring any oxygen bubbles were omitted and all vials were stirred continuously using small Teflon magnetic fleas to allow homogenous mixing of gases within the system during measurements. To improve the signal to noise ratio, seawater from each minicosm was concentrated above a 0.8 μm, 47 mm diameter polycarbonate membrane filter (Poretics) with gentle vacuum filtration and re-suspended in seawater from each minicosm CO_2 treatment. Each chamber was filled with the cell suspension and placed in a temperature controlled incubator (0.0 ± 0.5 °C). Light was supplied via fluorescent bulbs above each chamber and light intensity calibrated using a 4π sensor. Oxygen optode spots were connected to a FireSting O_2 logger and data acquired using FireSting software (PyroScience). The optode was calibrated according to the manufacturer's protocol immediately prior to measurements using a freshly prepared sodium thiosulfate solution (10% w/w) and agitated filtered seawater (0.2 μm) at experimental temperature for 0% and 100% air saturation values, respectively. Oxygen concentration was recorded until a linear change in rate was established for each pseudoreplicate (n = 4).

Measurements were first recorded in the light (188 μmol photons m^{-2} s^{-1}) and subsequently in the dark, with the initial steeper portion of the slope used for a linear regression analysis to determine post-illumination (PI) respiration rate. Gross community productivity (GCP$_{O_2}$) was then calculated from dark PI respiration (Resp$_{O_2}$) and net community production (NCP$_{O_2}$) rates and normalised to Chl *a* concentration (csGCP$_{O_2}$, Table 1). Chl *a* content for each concentrated sample was determined by extracting pigments in 90% chilled acetone and incubating in the dark at 4 °C for 24 hr. Chl *a* concentrations were determined using a spectrophotometer (Cary50:Varian) and calculated according to the equations of Jeffrey and Humphrey (1975), modified by Ritchie (2006).

2.10 Chlorophyll *a* fluorescence

Photosynthetic efficiency of the microalgal community was measured via Chl *a* fluorescence using a Pulse Amplitude Modulated fluorometer (Water PAM, Walz). A 3 ml aliquot from each minicosm was transferred into a quartz cuvette with continuous stirring to prevent cells from settling. To establish an appropriate dark adaptation period, several replicates were measured after 5, 10, 15, 20 and 30 min of dark adaptation, with the latter having the highest maximum quantum yield of PSII (F_v/F_m). Following dark adaptation, minimum fluorescence (F_0) was recorded before application of a high intensity saturating pulse of light (saturating pulse width = 0.8 s; saturating pulse intensity >3,000 μmol photons m^{-2} s^{-1}), where maximum fluo-

rescence (F_m) was determined. The maximum quantum yield of PSII was calculated from these two parameters (Schreiber, 2004). Following F_v/F_m, a five-step steady state light curve (SSLC) was conducted with each light level (130, 307, 600, 973, 1450 µmol photons $m^{-2}\,s^{-1}$) applied for 5 min before recording the light-adapted minimum (F_t) and maximum fluorescence ($F_{m'}$) values. Each light step was spaced by a 30 sec dark 'recovery' period, before the next light level was applied. Three

5   pseudoreplicate measurements were conducted on each minicosm sample at 0.1 °C. Non-photochemical quenching (NPQ) of Chl a fluorescence was calculated from F_m and $F_{m'}$ measurements. Relative electron transport rates (rETR) were calculated as the product of effective quantum yield ($\Delta F/F_{m'}$) and actinic irradiance (I_a). Calculations and units for each parameter are presented in Table 1.

2.11   Community carbon concentrating mechanism activity

10   To investigate the effects of CO_2 on carbon uptake, two inhibitors for carbonic anhydrase (CA) were applied to the 343 and 1641 µatm treatments on day 15: ethoxzolamide (EZA, Sigma), which inhibits both intracellular carbonic anhydrase (iCA) and extracellular carbonic anhydrase (eCA), and acetazolamide (AZA, Sigma), which blocks eCA only. Stock solutions of EZA (20 mM) and AZA (5 mM) were prepared in milliQ water, and the pH adjusted using NaOH to minimise pH changes when added to the samples. Before fluorometric measurements were made, water samples from the 343 and 1641 µatm CO_2 treatments were

15   filtered into $\geq$10 and $<$10 µm fractions and aliquots were inoculated either with 50 µl of milliQ water adjusted with $NaOH$ (control) or 50 µM final concentration of chemical inhibitor (EZA and AZA). Fluorescence measurements of size fractionated control- and inhibitor-exposed cells were performed using the Water-PAM. A 3 ml aliquot of sample was transferred into a quartz cuvette, with stirring, and left in the dark for 30 min before maximum quantum yield of PSII (F_v/F_m) was determined (as described above). Actinic light was then applied at 1450 µmol photons $m^{-2}\,s^{-1}$ for 5 min before effective quantum yield

20   of PSII ($\Delta F/F_{m'}$) was recorded. Three pseudoreplicate measurements were conducted on each minicosm sample at 0.1 °C.

2.12   Bacterial abundance

Bacterial abundance was determined daily using a Becton Dickinson FACScan or FACSCalibur flow cytometer fitted with a 488 nm laser following the protocol of Thomson et al. (2016). Samples were pre-filtered through a 50 µm mesh (Nitex), stored at 4 °C in the dark, and analysed within 6 hr of collection. Samples were stained for 20 min with 1:10,000 dilution SYBR-Green

25   I (Invitrogen) (Marie et al., 2005) and PeakFlow Green 2.5 µm beads (Invitrogen) were added to the sample as an internal fluorescence standard. Three pseudoreplicate samples were prepared from each minicosm seawater sample. Samples were run for 3 min at a low flow rate ($\sim$12 µl min^{-1}) and bacterial abundance was determined from side scatter (SSC) versus green (FL1) fluorescence bivariate scatter plots. The analysed volume was calibrated to the sample run time and each sample was run for precisely 3 min, resulting in an analysed volume of 0.0491 and 0.02604 ml on the FACSCalibur and FACScan, respectively.

30   The volume analysed was then used to calculate final cell concentrations.

2.13 Bacterial productivity

Bacterial productivity measurements were performed following the Leucine incorporation by microcentrifuge method of Kirchman (2001). Briefly, 70 nM ^{14}C-Leucine (PerkinElmer) was added to 1.7 ml seawater from each minicosm in 2 ml polyethylene Eppendorf tubes and incubated for 2 hr in the dark at 4 °C. Three pseudoreplicate samples were prepared from each minicosm

5 seawater sample. The reaction was terminated by the addition of 90 μl 100% trichloroacteic acid (TCA, Sigma) to each tube. Duplicate background controls were also performed following the same method, with 100% TCA added immediately before incubation. After incubation, samples were spun for 15 min at 12,500 rpm and the supernatant was removed. The cell pellet was resuspended into 1.7 ml ice-cold 5% TCA and spun again for 15 min at 12,500 rpm and the supernatant removed. The cell pellet was then resuspended into 1.7 ml ice-cold 80% ethanol, spun for a further 15 min at 12,500 rpm and the supernatant re-

10 moved. The cell pellet was allowed to dry completely before addition of 1 ml Ultima Gold scintillation cocktail (PerkinElmer). The Eppendorf tubes were placed into glass scintillation vials and DPMs were counted in a PerkinElmer Tri-Carb 2910TR Low Activity Liquid Scintillation Analyzer with a maximum counting time of 3 min.

DPM counts were converted to ^{14}C-Leucine incorporation rates following the equation in Kirchman (2001) and used to calculate gross bacterial production (GBP_{14C}), following Simon and Azam (1989). Bacterial production was divided by total

15 bacterial abundance to determine cell-specific bacterial productivity within each treatment ($csBP_{14C}$). Calculations and units for each parameter are presented in Table 1.

2.14 Statistical analysis

The minicosm experimental design measured the microbial community growth in six unreplicated $f\mathrm{CO}_2$ treatments. Therefore, sub-samples from each minicosm were within-treatment pseudoreplicates and thus, only provide a measure of the variability

20 of the within-treatment sampling and measurement procedures. We use pseudoreplicates as true replicates in order to provide an informal assessment of differences among treatments, noting that results must be treated as indicative and interpreted conservatively.

A linear or curved (quadratic) regression model was fitted to each CO_2 treatment over time using the *Stats* package in R (R Core Team, 2016) and an omnibus test of differences between the trends in productivity among CO_2 treatments over time was

25 assessed by ANOVA. This analysis ignored the repeated measures nature of the data set, which could not be modelled due to the low number of time points and an absence of replication at each time. For the CCM activity measurements, differences between treatments were tested by one-way ANOVA, followed by a post-hoc Tukey's test to determine which treatments differed. The significance level for all tests was set at < 0.05.

3 Results

3.1 Carbonate chemistry

The $f\mathrm{CO_2}$ of each treatment was modified in a step-wise fashion over 5 days to allow for acclimation of the microbial community to the changed conditions. Target treatment conditions were reached in all tanks by day 5, ranging from 343 to 1641 µatm, equating to an average pH_T of 8.1 to 7.45 (Fig. 2, Table S1), respectively. The initial seawater was calculated to have an $f\mathrm{CO_2}$ of 356 µatm and a PA of 2317 µmol kg^{-1}, from a measured pH_T of 8.08 and DIC of 2187 µmol kg^{-1} (Fig. S1, Table S2). One minicosm was maintained close to these conditions (343 µatm) throughout the experiment as a control treatment.

3.2 Light climate

The average light irradiance for all $\mathrm{CO_2}$ treatments is presented in Table S3. During the $\mathrm{CO_2}$ acclimation period (days 1-5) the average light irradiance was 0.9 ± 0.2 µmol photons m^{-2} s^{-1} and was increased to 90.5 ± 21.5 µmol photons m^{-2} s^{-1} by day 8. The average vertical light attenuation (K_d) across all minicosm tanks was 0.92 ± 0.2. Increasing Chl a concentration over time in all $\mathrm{CO_2}$ treatments increased $\mathrm{K}_{d(total)}$ from 0.96 ± 0.01 on day 1 to 3.53 ± 0.28 on day 18, resulting in a decline in average light irradiance within the minicosms from 86.61 ± 20.5 to 35.97 ± 9.3 µmol photons m^{-2} s^{-1} between days 8-18.

3.3 Nutrients

Nutrient concentrations were similar across all treatments at the beginning of the experiment (Table S2) and did not change during the acclimation period (days 1-5). Ammonia concentrations were initially low (0.95 ± 0.18 µM) and fell rapidly to concentrations below the limits of detection beyond day 12 in all treatments (Fig. S2). No differences in draw-down between $\mathrm{CO_2}$ treatments were observed, and thus it was excluded from further analysis. NOx fell from 26.2 ± 0.74 µM on day 8 to concentrations below detection limits on day 18 (Fig. 3a), with the slowest draw-down in the 1641 µatm treatment. SRP concentrations were initially 1.74 ± 0.02 µM and all $\mathrm{CO_2}$ treatments followed a similar draw-down sequence to NOx, reaching very low concentrations (0.13 µM) on day 18 in all treatments (Fig. 3b). In contrast, silica was replete in all treatments throughout the experiment falling from 60.0 ± 0.91 µM to 43.6 ± 2.45 µM (Fig. 3c). Draw-down of silica was exponential from day 8 onwards and followed a similar pattern to NOx and SRP, with the highest silica draw-down in the 634 µatm and the least in the 1641 µatm treatment.

3.4 Particulate organic matter

Particulate organic carbon (POC) and nitrogen (PON) concentrations were initially low, 4.7 ± 0.15 and 0.5 ± 0.98 µM respectively, and increased after day 8 in all treatments (Fig. 4a-b). The accumulation of POC and PON was effectively the reciprocal of the draw-down of nutrients (see above), being lowest in the high $\mathrm{CO_2}$ treatments ($\geq$1140 µatm) and highest in the 343 and 643 µatm treatments. Rates of POC and PON accumulation were both affected by nutrient exhaustion, with declines in the 343 and 634 µatm treatments between days 16 to 18. POC and PON concentrations on day 18 were highest in the 953 µatm

treatment. The ratio of POC to PON (C:N) was similar for all treatments, declining from 8.0 ± 0.38 on day 8 to 5.7 ± 0.28 on day 16 (Fig. 4c). The slowest initial decline in C:N ratio occurred in the 1641 µatm treatment, displaying a prolonged lag until day 10, after which it decreased to values similar to all other treatments. Nutrient exhaustion on day 18 coincided with an increase in the C:N ratio in all treatments, with C:N ratios >10 in the 343, 634, and 953 µatm treatments and lower C:N ratios

5   (8.6-6.7) in the 506, 1140, and 1641 µatm treatments.

3.5   Chlorophyll *a*

Chl *a* concentrations were low at the beginning of the experiment, 0.91 ± 0.16 µg l^{-1} and increased in all treatments after day 8 (Fig. 5a). Chl *a* accumulation rates were similar amongst treatments ≤634 µatm until day 14, with slightly higher Chl *a* concentration in the 506 and 634 µatm treatments on day 16 compared to the control treatment. By day 18, only the 503

10   µatm treatment remained higher than the control. Chl *a* accumulation rates in the 953 and 1140 µatm treatments were initially slow but increased after day 14, with Chl *a* concentrations similar to the control on days 16-18. The highest CO_2 treatment (1641 µatm) had the slowest rates of Chl *a* accumulation, displaying a lag in growth between days 8-12, after which Chl *a* concentration increased but remained lower than the control. Rates of Chl *a* accumulation slowed between days 16 and 18 in all treatments except 1641 µatm, coinciding with nutrient limitation. At day 18, the highest Chl *a* concentration was in the 506

15   µatm exposed treatment and lowest at 1641 µatm.

The omnibus test among CO_2 treatments of trends in Chl *a* over time indicated that the accumulation of Chl *a* in at least one treatment differed significantly from that of the control ($F_{5,23}$ = 5.45, p = 0.002; Table S4). Examination of individual coefficients from the model revealed that only the highest CO_2 treatment, 1641 µatm, was significantly different from the control at the 5% level.

20   ### 3.6 ^{14}C primary productivity

During the CO_2 and light acclimation phase of the experiment (days 1-8) all treatments displayed a steady decline in the maximum photosynthetic rate (P_{max}) and the maximum photosynthetic efficiency (α) to levels on day 8 approximately half of those at the beginning of the experiment, suggesting cellular acclimation to the light conditions (Fig. S3a-b). Thereafter, relative to the control, P_{max} and α were lowest in CO_2 levels ≥953 µatm and ≥634 µatm, respectively. Rates of photoinhibition (β)

25   and saturating irradiance (E_k) were variable and did not differ among treatments (Fig. S3c-d). The average E_k across all treatments was 28.7 ± 8.6 µmol photons m^{-2} s^{-1}, indicating that the light intensity in the minicosms was saturating for photosynthesis (see above) and not inhibiting ($\beta < 0.002$ mg C (mg Chl *a*)$^{-1}$ (µmol photons m^{-2} s^{-1})$^{-1}$ h^{-1}).

Chl *a*-specific primary productivity (csGPP$_{14C}$) and gross primary production (GPP$_{14C}$) was low during the CO_2 acclimation (days 1-5) and increased with increasing light climate after day 5. Rates of csGPP$_{14C}$ in treatments ≥634 µatm CO_2 were

30   consistently lower than the control between days 8-16, with the lowest rates in the highest CO_2 treatment (1641 µatm) (Fig. 6a). Rates of GPP$_{14C}$ in treatments ≤953 were similar between days 8-16, with the 343 (control), 506, and 953 µatm treatments increasing to 46.7 ± 0.34 µg C l^{-1} h^{-1} by day 18 (Fig. 5b). Compared to these treatments, GPP$_{14C}$ in the 634 µatm treatment

was lower on day 18, only reaching 39.7 µg C l^{-1} h^{-1}, possibly due to the concurrent limitation of NOx in this treatment on day 16 (see above).

The omnibus test among tanks of the trends in CO_2 treatments over time indicated that GPP$_{14C}$ in at least one treatment differed significantly from the control ($F_{5,23}$ = 4.95, p = 0.003; Table S5). Examination of the significance of individual curve terms revealed this manifested as differences between the 1140 and 1641 µatm treatments and the control group at the 5% level. No other curves were different from the control. In particular, GPP$_{14C}$ in the 1641 µatm treatment was much lower until day 12, after which it increased steadily until day 16. Between days 16-18, a substantial increase in GPP$_{14C}$ was observed in this treatment, subsequently resulting in a rate on day 18 that was similar to the 1140 µatm treatment (36.3 ± 0.08 µg C l^{-1} h^{-1}). Although, these treatments never reached rates of GPP$_{14C}$ as high as the control.

3.7   Gross community productivity

Productivity of the phytoplankton community increased over time in all CO_2 treatments, however there were clear differences in the timing and magnitude of this increase between treatments (Fig. 6b). A CO_2 effect was evident on day 12, where Chl a-normalised gross O_2 productivity rates (csGCP$_{O_2}$) increased with increasing CO_2 level, ranging from 19.5 - 248 mg O_2 (mg Chl a)$^{-1}$ h^{-1}. After day 12, the communities in CO_2 treatments ≤ 634 µatm continued to increase their rates of csGCP$_{O_2}$ until day 18 (97.7 ± 17.0 mg O_2 (mg Chl a)$^{-1}$ h^{-1}). The 953 and 1140 µatm CO_2 treatments peaked on day 12 (90.4 and 126 mg O_2 (mg Chl a)$^{-1}$ h^{-1}, respectively) and then declined on day 14 to rates similar to the control treatment. In contrast, the 1641 µatm treatment maintained high rates of csGCP$_{O_2}$ from days 12-14 (258 ± 13.8 mg O_2 (mg Chl a)$^{-1}$ h^{-1}), coinciding with the recovery of photosynthetic health (F$_v$/F$_m$, see below) and the initiation of growth in this treatment (see above). After this time, rates of csGCP$_{O_2}$ declined in this treatment to rates similar to the control. Despite these differences in csGCP$_{O_2}$, there was no significant difference between GCP$_{O_2}$ among CO_2 treatments (Fig. 5c).

3.8   Community photosynthetic efficiency

Community maximum quantum yield of PSII (F$_v$/F$_m$) showed a dynamic response over the duration of the experiment (Fig. 7). Values initially increased during the low light CO_2 adjustment period, but declined by day 8 when irradiance levels had increased. Between days 8-14, differences were evident in the photosynthetic health of the phytoplankton community across the CO_2 treatments, although by day 16 these differences had disappeared. Steady state light curves revealed that the community photosynthetic response did not change with increasing CO_2. Effective quantum yield of PSII (ΔF/F$_{m'}$) and NPQ showed no variability with CO_2 treatment (Fig. S5, S6). There was however, a notable decline in overall NPQ in all tanks with time, indicating an adjustment to the higher light conditions. Relative electron transport rates (rETR) showed differentiation with respect to CO_2 at high light (1450 µmol photons m^{-2} s^{-1}) on days 10-12. However, as seen with the F$_v$/F$_m$ response, this difference was diminished by day 18 (Fig. S7).

3.9 Community CCM activity

There was a significant decline in the effective quantum yield of PSII ($\Delta F/F_{m'}$) with the addition of the iCA and eCA inhibitor EZA to both the large (≥ 10 µm, p = 0.02) and small (< 10 µm, p < 0.001) size fractions of the phytoplankton community exposed to the control (343 µatm) CO_2 treatment (Fig. 8a). The addition of EZA to cells under high CO_2 (1641 µatm) had no effect on $\Delta F/F_{m'}$ for either size fraction. However, in the case of the small cells under high CO_2 (Fig. 8b), $\Delta F/F_{m'}$ was the same as that measured in the control CO_2 in the presence of EZA. The addition of AZA, which inhibits eCA only, had no effect for either CO_2 treatments in the large celled community. In contrast, there was a significant decline in $\Delta F/F_{m'}$ in the smaller fraction in the control CO_2 treatment (p < 0.001), but no effect of AZA addition under high CO_2. Again, the high CO_2 cells exhibited the same $\Delta F/F_{m'}$ as those measured under the control CO_2 in the presence of AZA.

3.10 Bacterial abundance

During the 8 day acclimation period, bacterial abundance in treatments ≥ 634 µatm increased with increasing CO_2, reaching 26.0-32.4 x 10^7 cells l^{-1}, and remaining high until day 13 (Fig. 9a). Between days 7-13, bacterial abundances in CO_2 treatments ≥ 953 were higher than the control. In contrast, abundance remained constant in treatments ≤ 506 µatm (20.6 $\pm$ 1.4 x 10^7 cells l^{-1}) until day 11. Cell numbers rapidly declined in all treatments after day 12, finally stabilising at 0.5 $\pm$ 0.2 x 10^7 cells l^{-1}. An omnibus test among CO_2 treatments of the trends in bacterial abundance over time showed that changes in abundance in at least one treatment differed significantly from the control ($F_{5,185}$ = 9.78, p < 0.001; Table S6). Examination of individual coefficients from the model revealed that CO_2 treatments ≥ 953 µatm were significantly different from the control at the 5% level.

3.11 Bacterial productivity

Gross bacterial production (GBP$_{14C}$) was low in all CO_2 treatments (0.2 $\pm$ 0.03 µg C l^{-1} h^{-1}) and changed little during the first 5 days of incubation (Fig. 9b). Thereafter it increased, coinciding with exponential growth in the phytoplankton community. The most rapid increase in GBP$_{14C}$ was observed in the 634 µatm treatment, resulting in a rate twice that of all other treatments by day 18 (2.1 µg C l^{-1} h^{-1}). No difference was observed among other treatments, all of which increased to an average rate of 1.1 $\pm$ 0.1 µg C l^{-1} h^{-1} by day 18. Cell-specific bacterial productivity (csBP$_{14C}$) was low in all treatments (1.2 $\pm$ 0.5 fg C l^{-1} h^{-1}) until day 14, with slower rates in treatments ≥ 953 µatm, likely due to high cell abundances observed in these treatments (Fig. S8). It then increased from day 14, coinciding with a decline in bacterial abundance. Rates of csBP$_{14C}$ did not differ among treatments until day 18, when the rate in the 634 µatm treatment was higher than all other treatments (0.5 pg C cell^{-1} l^{-1} h^{-1}).

4   Discussion

Our study of a natural Antarctic phytoplankton community identified a critical threshold for tolerance of CO_2 between 953 and 1140 µatm, above which photosynthetic health was negatively affected and rates of carbon fixation and Chl a accumulation declined. Low rates of primary productivity also led to declines in nutrient uptake rates and POM production, although there was no effect of CO_2 on C:N ratios, indicating that ocean acidification effects on the phytoplankton community did not modify POM stoichiometry. Assessing the temporal trends of Chl a, GPP_{14C}, and PON against CO_2 treatment revealed that the downturn in these parameters occurred between 634 and 953 µatm fCO_2 and could be discerned following ≥ 12 days incubation (Fig. 10). On the final day of the experiment (day 18), this CO_2 threshold was less clear and likely confounded by the effects of nutrient limitation (Westwood et al., submitted). In contrast, bacterial productivity was unaffected by increased CO_2. Instead, their production coincided with increased organic matter supply from phytoplankton primary productivity. In the following sections these effects will be investigated further, with suggestions for possible mechanisms that may be driving the responses observed.

4.1   Ocean acidification effects on phytoplankton productivity

The results of this study suggest that exposing phytoplankton to high CO_2 levels can decouple the two stages of photosynthesis (but also see discussion below). At CO_2 levels ≥ 1140 µatm, Chl a-specific oxygen production ($csGCP_{O_2}$) increased strongly yet displayed the lowest rates of Chl a-specific carbon fixation ($csGPP_{14C}$, Fig. 6). This mismatch in oxygen production and carbon fixation is likely due to the two-stage process in the photosynthetic fixation of carbon (reviewed in Behrenfeld et al., 2004). In the first stage, light-dependent reactions occur within the chloroplast, converting light energy (photons) into the cellular energy products, adenosine triphosphate (ATP) and nicotinamide adenine dinucleotide phosphate (NADPH), producing O_2 as a by-product. This cellular energy is then utilised in a second, light-independent pathway, which uses the carbon-fixing enzyme RuBisCo to convert CO_2 into sugars through the Calvin Cycle. However, under certain circumstances the relative pool of energy may also be consumed in alternative pathways, such as respiration and photoprotection (Behrenfeld et al., 2004; Gao and Campbell, 2014). Increases in energy requirements for these alternate pathways have been demonstrated, where measurements of maximum photosynthetic rates (P_{max}) and photosynthetic efficiency (α) display changes that result in no change to saturating irradiance levels (E_k) (Behrenfeld et al., 2004, 2008; Halsey et al., 2010). This "E_k-independent variability" was evident in our study, where decreases in P_{max} and α were observed in the high CO_2 treatments, while E_k remained unaffected (Fig. S3).

This highlights an important tipping point in the phytoplankton community's ability to cope with the energetic requirements for maintaining efficient productivity under high CO_2. While studies on individual phytoplankton species have reported decoupling of the photosynthetic pathway under conditions of stress, to date, no studies on natural phytoplankton communities have reported this response. Under laboratory conditions, stresses such as nutrient limitation (Halsey et al., 2010) or a combination of high CO_2 and light climate (Hoppe et al., 2015; Liu et al., 2017) have been shown to induce such a response, where isolated phytoplankton species possess higher energy requirements for carbon fixation. In our study, the phytoplankton community

experienced a dynamic light climate due to continuous gentle mixing of the minicosm contents, and although nutrients weren't limiting, the phytoplankton in the higher CO_2 treatments did show lower $csGPP_{14C}$ rates (Fig. 6a), which could be linked to higher energy demand for light-independent processes. Since nutrients were replete and not a likely source of stress, it follows that CO_2 and light were likely the only sources of stress on this community.

5   Increased respiration rates could account for the decreased carbon fixation rates measured. Thus far, respiration rates are commonly reported as either unaffected or lower under increasing CO_2 (Hennon et al., 2014; Trimborn et al., 2014; Spilling et al., 2016). This effect is generally attributed to declines in cellular energy requirements, via processes such as down-regulation of CCMs, which can result in observed increases to rates of production (Spilling et al., 2016). Despite this, decreased growth rates have been linked to enhanced respiratory carbon loss at high CO_2 levels (800-1000 µatm) (Gao et al., 2012b). The

10   contribution of community respiration rates to $csGCP_{O_2}$ was high and increased with increasing CO_2 (Fig. S4). However, respiration rates were generally proportional to the increase in O_2 production (i.e, the ratio of production to respiration remained constant across CO_2 conditions), making it unlikely to be a significant contributor to the decline in carbon fixation. Instead, high respiration rates were possibly a result of heterotrophic activity.

     It has been suggested that the negative effects of ocean acidification are predominantly due to the decline in pH and not

15   the increase in CO2 concentration (e.g. McMinn et al., 2014; Coad et al., 2016). A decline in pH with ocean acidification increases the hydrogen ion (H^+) concentration in the seawater and is likely to make it increasingly difficult for phytoplankton cells to maintain cellular homeostasis. Metabolic processes, such as photosynthesis and respiration, impact on cellular H^+ fluxes between compartments, making it necessary to temporarily balance internal H^+ concentrations through H^+ channels Taylor2012. Under normal oceanic conditions (pH ~8.1), when the extracellular environment is above pH 7.8, excess H^+

20   ions generated within the cell are able to passively diffuse out of the cell through these H^+ channels. However, a lowering of the oceanic pH below 7.8 is likely to halt this passive removal of internal H^+, requiring the utilisation of energy-intensive proton pumps (Taylor et al., 2012), and thus potentially reducing the energy pool available for carbon fixation. While not well understood, these H^+ channels may also perform important cellular functions, such as nutrient uptake, cellular signalling, and defense (Taylor et al., 2012). Our results are consistent with this idea of a critical pH threshold, as significant declines in

25   GPP_{14C} were observed in treatments $\geq$1140 µatm (Fig. 10), the CO_2 treatments where the pH ranged from 7.69-7.45 (Fig. 2).

     Despite the initial stress of high CO_2 between days 8-12, the phytoplankton community displayed a strong ability to adapt to these conditions. The CO_2-induced reduction in F_v/F_m showed a steady recovery between days 12 and 16, with all treatments displaying similar high F_v/F_m at day 16 (0.68-0.71). This recovery in photosynthetic health suggests that the phytoplankton community was able to acclimate to the high CO_2 conditions, possibly through cellular acclimation, changes in community

30   structure, or most likely, a combination of both. Cellular acclimations were observed in our study. A lowering of NPQ and a minimisation of the CO_2-related response to photoinhibition (rETR) at high light intensity suggested that PSII was being down-regulated to adjust to a higher light climate (Fig. S6, S7). Decreased energy requirements for carbon fixation were also observed in the photosynthetic pathway, resulting in increases to GPP_{14C} and Chl *a* accumulation rates (Fig. 5). Acclimation to increased CO_2 has been reported in a number of studies, resulting in shifts in carbon and energy utilisation (Sobrino et al.,

35   2008; Hopkinson et al., 2010; Hennon et al., 2014; Trimborn et al., 2014; Zheng et al., 2015). Numerous photophysiological

investigations on individual phytoplankton species also report species-specific tolerances to increased CO_2 (Gao et al., 2012a; Gao and Campbell, 2014; Trimborn et al., 2013, 2014) and a general trend toward smaller-celled communities with increased CO_2 has been reported in ocean acidification studies globally (Schulz et al., 2017). Changes in community structure were observed with increasing CO_2, with taxon-specific thresholds of CO_2 tolerance (Hancock et al., submitted). Within the diatom

5 community, the response was also related to size, leading to an increase in abundance of small (<20 μm) diatoms in the higher CO_2 treatments (≥ 953 μatm). Therefore, the community acclimation observed is likely driven by an increase in growth of more tolerant species.

It is often suggested that the down-regulation of CCMs help to moderate the sensitivity of phytoplankton communities to increasing CO_2. The carbon-fixing enzyme RubisCO has a low affinity for CO_2 that is compensated for through CCMs that

10 actively increase the intracellular CO_2 (Raven, 1991; Badger, 1994; Badger et al., 1998; Hopkinson et al., 2011). This process requires additional cellular energy (Raven, 1991) and numerous studies have suggested that the energy savings from down-regulation of CCMs in phytoplankton could explain increases in rates of primary productivity at elevated CO_2 levels (Tortell et al., 2000; Tortell and Morel, 2002; Cassar et al., 2004; Tortell et al., 2008b, 2010; Trimborn et al., 2013; Young et al., 2015). In Antarctic phytoplankton communities, Young et al. (2015) showed that the energetic costs of CCMs are low and

15 any down-regulation at increased CO_2 would provide little benefit. We found that the CCM component carbonic anhydrase (CA) was utilised by the phytoplankton community at our control CO_2 level (343 μatm), and was down-regulated at high CO_2 (1641 μatm, Fig. 8). Yet we saw no promotion of primary productivity that coincided with this down-regulation. Thus, our data support the previous studies showing that increased CO_2 may alleviate energy supply constraints but does not necessarily lead to increased rates of carbon fixation (Rost et al., 2003; Cassar et al., 2004; Riebesell, 2004).

20 Furthermore, size-specific differences in phytoplankton CCM utilisation were observed. The absence of eCA activity in the large phytoplankton (≥ 10 μm, Fig. 8a) suggests that bicarbonate (HCO_3^-) was the dominant carbon source used by this fraction of the phytoplankton community (Burkhardt et al., 2001; Tortell et al., 2008a). This is not surprising as direct HCO_3^- uptake has been commonly reported among Antarctic phytoplankton communities (Cassar et al., 2004; Tortell et al., 2008a, 2010). On the other hand, the small phytoplankton (<10 μm, Fig. 8b) seem to have used both iCA and eCA, implying carbon

25 for photosynthesis was sourced through both extracellular conversion of HCO_3^- to CO_2 and direct HCO_3^- uptake (Rost et al., 2003). Despite these patterns, CCM activity in this study was only determined via Chl *a* fluorescence, and therefore direct measurement of light-dependent reactions in photosynthesis. This imposes limitations to the interpretability of this particular data set, as CA is involved primarily in carbon acquisition, which occurs during photosynthetic reactions that are independent of light.

30 The presence of iCA has also been proposed as a possible mechanism for increased sensitivity of phytoplankton to decreased pH conditions. Satoh et al. (2001) found that the presence of iCA caused strong intracellular acidification and inhibition of carbon fixation when a CO_2-tolerant iCA-expressing algal species was transferred from ambient conditions to very high CO_2 (40%). Down-regulation of iCA through acclimation in a 5% CO_2 treatment eliminated this response, with similar tolerance observed in an algal species with low ambient iCA activity. Thus, the down-regulation of iCA activity at high CO_2, as was seen

17

in our study, may not only decrease cellular energy demands but may also be operating as a cellular protection mechanism, allowing the cell to maintain intracellular homeostasis.

Contrary to the high CO_2 treatments, the phytoplankton community appeared to tolerate CO_2 levels up to 953 µatm, identifying a CO_2 threshold. Between days 8-14 we observed a small and insignificant CO_2-related decline in F_v/F_m, GPP_{14C}, and Chl a accumulation between the 343-953 µatm treatments (Fig. 7, 10). Tolerance of CO_2 levels up to ∼1000 µatm has often been observed in natural phytoplankton communities in regions exposed to fluctuating CO_2 levels. In these communities, increasing CO_2 often had no effect on primary productivity (Tortell et al., 2000; Tortell and Morel, 2002; Tortell et al., 2008b; Hopkinson et al., 2010; Tanaka et al., 2013; Sommer et al., 2015; Young et al., 2015; Spilling et al., 2016) or growth (Tortell et al., 2008b; Schulz et al., 2013), although an increase in primary production has been observed in some instances (Riebesell, 2004; Tortell et al., 2008b; Egge et al., 2009; Tortell et al., 2010; Hoppe et al., 2013; Holding et al., 2015). These differing responses may be due to differences in community composition, nutrient supply, or ecological adaptations of the phytoplankton community in the region studied. They may also be due to differences in the experimental methods, especially the range of CO_2 concentrations employed (Hancock et al., submitted); the mechanism used to manipulate CO_2 concentrations; the duration of the acclimation and incubation; the nature and volume of the mesocosms used; and the extent to which higher trophic levels are screened from the mesocosm contents (see Davidson et al., 2016).

Previous studies in Prydz Bay report a tolerance of the phytoplankton community to CO_2 levels up to 750 µatm (Davidson et al., 2016; Thomson et al., 2016; Westwood et al., submitted). Although these experiments differed in nutrient concentration, community composition, and CO_2 manipulation from ours, when taken together, these studies demonstrate consistent CO_2 effects throughout the Antarctic summer season and across years in this location. The most likely reason for this high tolerance is that these communities are already exposed to highly variable CO_2 conditions. CO_2 naturally builds beneath the sea ice in winter, when primary productivity is low (Perrin et al., 1987; Legendre et al., 1992), and is rapidly depleted during spring and summer by phytoplankton blooms, resulting in annual fCO_2 fluctuations between ∼50-500 µatm (Gibson and Trull, 1999; Roden et al., 2013). Thus, variable CO_2 environments appear to promote adaptations within the phytoplankton community to manage the stress imposed by fluctuating CO_2.

Changes in POM production and C:N ratio in phytoplankton communities can have significant effects on carbon sequestration and change their nutritional value for higher trophic levels (Finkel et al., 2010; van de Waal et al., 2010; Polimene et al., 2016). We observed a decline in particulate organic matter production (POM) at CO_2 levels ≥1140 µatm (Fig. 10), while changes in organic matter stoichiometry (C:N ratio) appeared to be predominantly controlled by nutrient consumption (Fig. 4). Increases in POM production were similar to Chl a accumulation, with declines in high CO_2 treatments (≥1140µatm) due to low rates of primary productivity. Carbon overconsumption has been reported in some natural phytoplankton communities exposed to increased CO_2, resulting in observed or inferred increases in the particulate C:N ratio (Riebesell et al., 2007; Engel et al., 2014). While in our study the C:N ratio did decline to below the Redfield Ratio during exponential growth, it remained within previously reported C:N ratios of coastal phytoplankton communities in this region (Gibson and Trull, 1999; Pasquer et al., 2010). However, as we did not analyse the elemental composition of dissolved inorganic matter, carbon overconsumption cannot be completely ruled out (Kähler and Koeve, 2001). Therefore, it is difficult to say whether or not changes in primary pro-

ductivity will affect organic matter stoichiometry in this region, particularly as any resultant long-term changes in community composition to more CO2-tolerant taxa may also have an effect (Finkel et al., 2010).

4.2   Ocean acidification effects on bacterial productivity

In contrast to the phytoplankton community, bacteria were tolerant of high CO_2 levels. The low bacterial productivity and abundance of the initial community is characteristic of the post-winter bacterial community in Prydz Bay where their growth is limited by organic nutrient availability (Pearce et al., 2007). Whilst an increase in cell abundance was observed at CO_2 levels ≥ 634 µatm (Fig. 9a), it was possible that this response was driven by a decline in grazing by heterotrophs (Thomson et al., 2016; Westwood et al., submitted) instead of a direct CO_2-related promotion in bacterial growth. The subsequent decline in abundance was likely due to top-down control from the heterotrophic nanoflagellate community, which displayed an increase in abundance at this time (Hancock et al., submitted). Bacterial tolerance to high CO_2 has been reported previously in this region (Thomson et al., 2016; Westwood et al., submitted) and has also been reported in numerous studies in the Arctic (Grossart et al., 2006; Allgaier et al., 2008; Paulino et al., 2008; Baragi et al., 2015; Wang et al., 2016), suggesting that the marine bacterial community will be resilient to increasing CO_2.

While we detected an increase in bacterial productivity, this response appeared to be correlated with an increase in Chl *a* concentration and available POM, rather than CO_2. Bacterial productivity was similar among all CO_2 treatments, except for a final promotion of productivity at 634 µatm on day 18 (Fig. 9b). This promotion of growth may be linked to an increase in diatom abundance observed in this treatment (Hancock et al., submitted). The coupling of bacterial growth with phytoplankton productivity has been reported by numerous studies on natural marine microbial communities (Allgaier et al., 2008; Grossart et al., 2006; Engel et al., 2013; Piontek et al., 2013; Sperling et al., 2013; Bergen et al., 2016). Thus, it is likely that the bacterial community was controlled more by grazing and nutrient availability than by CO_2 level.

5   Conclusions

These results support the identification of a tipping point in the marine microbial community response to CO_2 between 953 and 1140 µatm. When exposed to CO_2 ≥ 634 µatm, declines in growth rates, primary productivity, and organic matter production were observed in the phytoplankton community and became significantly different when ≥ 1140 µatm. Despite this, the community displayed the ability to adapt to these high CO_2 conditions, down-regulating CCMs and likely adjusting other intracellular mechanisms to cope with the added stress of low pH. However, the lag in growth and subsequent acclimation to high CO_2 conditions allowed for more tolerant species to thrive (Hancock et al., submitted).

Conditions in Antarctic coastal regions fluctuate throughout the seasons and the marine microbial community is already tolerant to changes in CO_2 level, light availability, and nutrients (Gibson and Trull, 1999; Roden et al., 2013). It is possible that phytoplankton communities already exposed to highly variable conditions will be more capable of adapting to the projected changes in CO_2 (Schaum and Collins, 2014; Boyd et al., 2016). Although, this will likely also include adaptation at the community level, causing a shift in dominance to more tolerant species. This has been observed in numerous ocean acidification

experiments, with a trend in community composition favouring picophytoplankton and away from large diatoms (Davidson et al., 2016; Reviewed in Schulz et al., 2017). Such a change in phytoplankton community composition may have flow on effects to higher trophic levels that feed on Antarctic phytoplankton blooms. It could also have a significant effect on the biological pump, with decreased carbon draw-down at high CO_2, causing a negative feedback on anthropogenic CO_2 uptake.

5 Coincident increases in bacterial abundance under high CO_2 conditions may also increase the efficiency of the microbial loop, resulting in increased organic matter remineralisation and further declines in carbon sequestration.

References

Allgaier, M., Riebesell, U., Vogt, M., Thyrhaug, R., and Grossart, H.-P.: Coupling of heterotrophic bacteria to phytoplankton bloom development at different pCO_2 levels: a mesocosm study, Biogeosciences, 5, 1007–1022, doi:10.5194/bg-5-1007-2008, 2008.

Arrigo, K. R., van Dijken, G. L., and Bushinsky, S.: Primary production in the Southern Ocean, 1997-2006, J. Geophys. Res. Ocean., 113, C08 004, doi:10.1029/2007JC004551, 2008a.

Arrigo, K. R., van Dijken, G. L., and Long, M.: Coastal Southern Ocean: A strong anthropogenic CO_2 sink, Geophys. Res. Lett., 35, L21 602, doi:10.1029/2008GL035624, 2008b.

Azam, F., Fenchel, T., Field, J. G., Gray, J. C., Meyer-Reil, L. A., and Thingstad, F.: The ecological role of water-column microbes in the sea, Mar. Ecol. Prog. Ser., 10, 257–264, doi:10.3354/meps010257, 1983.

Azam, F., Smith, D. C., and Hollibaugh, J. T.: The role of the microbial loop in Antarctic pelagic ecosystems, Polar Res., 10, 239–243, doi:10.1111/j.1751-8369.1991.tb00649.x, 1991.

Bach, L. T., Taucher, J., Boxhammer, T., Ludwig, A., Achterberg, E. P., Algueró-Muñiz, M., Anderson, L. G., Bellworthy, J., Büdenbender, J., Czerny, J., Ericson, Y., Esposito, M., Fischer, M., Haunost, M., Hellemann, D., Horn, H. G., Hornick, T., Meyer, J., Sswat, M., Zark, M., and Riebesell, U.: Influence of ocean acidification on a natural winter-to-summer plankton succession first insights from a long-term mesocosm study draw attention to periods of low nutrient concentrations, PLoS One, 11, e0159 068, doi:10.1371/journal.pone.0159068, 2016.

Badger, M.: The Role of Carbonic Anhydrase in Photosynthesis, Annu. Rev. Plant Physiol. Plant Mol. Biol., 45, 369–392, doi:10.1146/annurev.arplant.45.1.369, 1994.

Badger, M. R., Andrews, T. J., Whitney, S., Ludwig, M., Yellowlees, D. C., Leggat, W., and Price, G. D.: The diversity and coevolution of Rubisco, plastids, pyrenoids, and chloroplast-based CO_2-concentrating mechanisms in algae, Can. J. Bot., 76, 1052–1071, doi:10.1139/cjb-76-6-1052, 1998.

Baragi, L. V., Khandeparker, L., and Anil, A. C.: Influence of elevated temperature and pCO_2 on the marine periphytic diatom *Navicula distans* and its associated organisms in culture, Hydrobiologia, 762, 127–142, doi:10.1007/s10750-015-2343-9, 2015.

Barcelos e Ramos, J., Schulz, K. G., Brownlee, C., Sett, S., and Azevedo, E. B.: Effects of Increasing Seawater Carbon Dioxide Concentrations on Chain Formation of the Diatom *Asterionellopsis glacialis*, PLoS One, 9, e90 749, doi:10.1371/journal.pone.0090749, 2014.

Behrenfeld, M. J., Prasil, O., Babin, M., and Bruyant, F.: In Search of a Physiological Basis for Covariations in Light-Limited and Light-Saturated Photosynthesis, J. Phycol., 40, 4–25, doi:10.1046/j.1529-8817.2004.03083.x, 2004.

Behrenfeld, M. J., Halsey, K. H., and Milligan, A. J.: Evolved physiological responses of phytoplankton to their integrated growth environment., Philos. Trans. R. Soc. B, 363, 2687–2703, doi:10.1098/rstb.2008.0019, 2008.

Bellerby, R. G. J., Schulz, K. G., Riebesell, U., Neill, C., Nondal, G., Heegaard, E., Johannessen, T., and Brown, K. R.: Marine ecosystem community carbon and nutrient uptake stoichiometry under varying ocean acidification during the PeECE III experiment, Biogeosciences, 5, 1517–1527, doi:10.5194/bg-5-1517-2008, 2008.

Berge, T., Daugbjerg, N., Balling Andersen, B., and Hansen, P.: Effect of lowered pH on marine phytoplankton growth rates, Mar. Ecol. Prog. Ser., 416, 79–91, doi:10.3354/meps08780, 2010.

Bergen, B., Endres, S., Engel, A., Zark, M., Dittmar, T., Sommer, U., and Jürgens, K.: Acidification and warming affect prominent bacteria in two seasonal phytoplankton bloom mesocosms, Environ. Microbiol., 18, 4579–4595, doi:10.1111/1462-2920.13549, http://doi.wiley.com/10.1111/1462-2920.13549, 2016.

Bi, R., Ismar, S., Sommer, U., and Zhao, M.: Environmental dependence of the correlations between stoichiometric and fatty acid-based indicators of phytoplankton nutritional quality, Limnol. Oceanogr., 62, 334–347, doi:10.1002/lno.10429, 2017.

Bockmon, E. E. and Dickson, A. G.: A seawater filtration method suitable for total dissolved inorganic carbon and pH analyses, Limnol. Oceanogr. Methods, 12, 191–195, doi:10.4319/lom.2014.12.191, 2014.

5 Boyd, P. W., Doney, S. C., Strzepek, R., Dusenberry, J., Lindsay, K., and Fung, I.: Climate-mediated changes to mixed-layer properties in the Southern Ocean: assessing the phytoplankton response, Biogeosciences, 5, 847–864, doi:10.5194/bg-5-847-2008, 2008.

Boyd, P. W., Cornwall, C. E., Davidson, A., Doney, S. C., Fourquez, M., Hurd, C. L., Lima, I. D., and McMinn, A.: Biological responses to environmental heterogeneity under future ocean conditions, Glob. Chang. Biol., 22, 2633–2650, doi:10.1111/gcb.13287, 2016.

Bunse, C., Lundin, D., Karlsson, C. M. G., Vila-Costa, M., Palovaara, J., Akram, N., Svensson, L., Holmfeldt, K., González, J. M., Calvo,

10 E., Pelejero, C., Marrasé, C., Dopson, M., Gasol, J. M., and Pinhassi, J.: Response of marine bacterioplankton pH homeostasis gene expression to elevated CO_2, Nat. Clim. Chang., 1, 1–7, doi:10.1038/nclimate2914, 2016.

Burkhardt, S., Amoroso, G., Riebesell, U., and Sültemeyer, D.: CO_2 and HCO_3^- uptake in marine diatoms acclimated to different CO_2 concentrations, Limnol. Oceanogr., 46, 1378–1391, doi:10.4319/lo.2001.46.6.1378, 2001.

Caldeira, K. and Wickett, M. E.: Oceanography: Anthropogenic carbon and ocean pH, Nature, 425, 365–365, doi:10.1038/425365a, 2003.

15 Cassar, N., Laws, E. A., Bidigare, R. R., and Popp, B. N.: Bicarbonate uptake by Southern Ocean phytoplankton, Global Biogeochem. Cycles, 18, 1–10, doi:10.1029/2003GB002116, 2004.

Chen, C. and Durbin, E.: Effects of pH on the growth and carbon uptake of marine phytoplankton, Mar. Ecol. Prog. Ser., 109, 83–94, doi:10.3354/meps109083, 1994.

Chen, H., Guan, W., Zeng, G., Li, P., and Chen, S.: Alleviation of solar ultraviolet radiation (UVR)-induced photoinhibition in diatom

20 *Chaetoceros curvisetus* by ocean acidification, J. Mar. Biol. Assoc. United Kingdom, 95, 661–667, doi:10.1017/S0025315414001568, 2015.

Coad, T., McMinn, A., Nomura, D., and Martin, A.: Effect of elevated CO2 concentration on microalgal communities in Antarctic pack ice, Deep Sea Res. Part II Top. Stud. Oceanogr., 131, 160–169, doi:10.1016/j.dsr2.2016.01.005, 2016.

Davidson, A., McKinlay, J., Westwood, K., Thomson, P., van den Enden, R., de Salas, M., Wright, S., Johnson, R., and Berry, K.:

25 Enhanced CO_2 concentrations change the structure of Antarctic marine microbial communities, Mar. Ecol. Prog. Ser., 552, 93–113, doi:10.3354/meps11742, 2016.

Deppeler, S. L. and Davidson, A. T.: Southern Ocean Phytoplankton in a Changing Climate, Front. Mar. Sci., 4, 40, doi:10.3389/fmars.2017.00040, 2017.

Dickson, A.: Standards for Ocean Measurements, Oceanography, 23, 34–47, doi:10.5670/oceanog.2010.22, 2010.

30 Dickson, A., Sabine, C., and Christian, J., eds.: Guide to Best Practices for Ocean CO_2 Measurements, North Pacific Marine Science Organization, Sidney, British Columbia, 2007.

Dring, M. J. and Jewson, D. H.: What Does 14C Uptake by Phytoplankton Really Measure? A Theoretical Modelling Approach, Proc. R. Soc. B Biol. Sci., 214, 351–368, doi:10.1098/rspb.1982.0016, 1982.

Ducklow, H. W., Baker, K., Martinson, D. G., Quetin, L. B., Ross, R. M., Smith, R. C., Stammerjohn, S. E., Vernet, M., and Fraser, W.:

35 Marine pelagic ecosystems: the West Antarctic Peninsula, Philos. Trans. R. Soc. B Biol. Sci., 362, 67–94, doi:10.1098/rstb.2006.1955, 2007.

Egge, J. K., Thingstad, T. F., Larsen, A., Engel, A., Wohlers, J., Bellerby, R. G. J., and Riebesell, U.: Primary production during nutrient-induced blooms at elevated CO_2 concentrations, Biogeosciences, 6, 877–885, doi:10.5194/bg-6-877-2009, 2009.

Engel, A., Borchard, C., Piontek, J., Schulz, K. G., Riebesell, U., and Bellerby, R.: CO_2 increases ^{14}C primary production in an Arctic plankton community, Biogeosciences, 10, 1291–1308, doi:10.5194/bg-10-1291-2013, 2013.

Engel, A., Piontek, J., Grossart, H.-P., Riebesell, U., Schulz, K. G., and Sperling, M.: Impact of CO_2 enrichment on organic matter dynamics during nutrient induced coastal phytoplankton blooms, J. Plankton Res., 36, 641–657, doi:10.1093/plankt/fbt125, 2014.

5   Fabry, V., McClintock, J., Mathis, J., and Grebmeier, J.: Ocean Acidification at High Latitudes: The Bellwether, Oceanography, 22, 160–171, doi:10.5670/oceanog.2009.105, 2009.

Fenchel, T.: The microbial loop - 25 years later, J. Exp. Mar. Bio. Ecol., 366, 99–103, doi:10.1016/j.jembe.2008.07.013, 2008.

Feng, Y., Hare, C., Rose, J., Handy, S., DiTullio, G., Lee, P., Smith, W. J., Peloquin, J., Tozzi, S., Sun, J., Zhang, Y., Dunbar, R., Long, M., Sohst, B., Lohan, M., and Hutchins, D.: Interactive effects of iron, irradiance and CO_2 on Ross Sea phytoplankton, Deep Sea Res. Part I
10   Oceanogr. Res. Pap., 57, 368–383, doi:10.1016/j.dsr.2009.10.013, 2010.

Finkel, Z. V., Beardall, J., Flynn, K. J., Quigg, A., Rees, T. A. V., and Raven, J. A.: Phytoplankton in a changing world: cell size and elemental stoichiometry, J. Plankton Res., 32, 119–137, doi:10.1093/plankt/fbp098, 2010.

Frölicher, T. L., Sarmiento, J. L., Paynter, D. J., Dunne, J. P., Krasting, J. P., and Winton, M.: Dominance of the Southern Ocean in Anthropogenic Carbon and Heat Uptake in CMIP5 Models, J. Clim., 28, 862–886, doi:10.1175/JCLI-D-14-00117.1, 2015.

15   Gao, K. and Campbell, D. A.: Photophysiological responses of marine diatoms to elevated CO_2 and decreased pH: a review, Funct. Plant Biol., 41, 449–459, doi:10.1071/FP13247, 2014.

Gao, K., Helbling, E., Häder, D., and Hutchins, D.: Responses of marine primary producers to interactions between ocean acidification, solar radiation, and warming, Mar. Ecol. Prog. Ser., 470, 167–189, doi:10.3354/meps10043, 2012a.

Gao, K., Xu, J., Gao, G., Li, Y., Hutchins, D. A., Huang, B., Wang, L., Zheng, Y., Jin, P., Cai, X., Häder, D.-p., Li, W., Xu, K., Liu, N.,
20   and Riebesell, U.: Rising CO_2 and increased light exposure synergistically reduce marine primary productivity, Nat. Clim. Chang., 2, 519–523, doi:10.1038/nclimate1507, 2012b.

Gattuso, J.-P., Gao, K., Lee, K., Rost, B., and Schulz, K. G.: Approaches and tools to manipulate the carbonate chemistry, in: Guide to best practices for ocean acidification research and data reporting, edited by Riebesell, U., Fabry, V. J., Hansson, L., and Gattuso, J.-P., chap. 2, pp. 41–52, Publications Office of the European Union, Luxembourg, doi:10.2777/66906, 2010.

25   Gibson, J. A. and Trull, T. W.: Annual cycle of $f CO_2$ under sea-ice and in open water in Prydz Bay, East Antarctica, Mar. Chem., 66, 187–200, doi:10.1016/S0304-4203(99)00040-7, 1999.

González, N., Gattuso, J. P., and Middelburg, J. J.: Oxygen production and carbon fixation in oligotrophic coastal bays and the relationship with gross and net primary production, Aquat. Microb. Ecol., 52, 119–130, doi:10.3354/ame01208, 2008.

Grossart, H.-P., Allgaier, M., Passow, U., and Riebesell, U.: Testing the effect of CO_2 concentration on the dynamics of marine heterotrophic
30   bacterioplankton, Limnol. Oceanogr., 51, 1–11, doi:10.4319/lo.2006.51.1.0001, 2006.

Halsey, K. H., Milligan, A. J., and Behrenfeld, M. J.: Physiological optimization underlies growth rate-independent chlorophyll-specific gross and net primary production, Photosynth. Res., 103, 125–137, doi:10.1007/s11120-009-9526-z, 2010.

Hancock, A., Davidson, A., McKinlay, J., McMinn, A., Schulz, K., and van den Enden, R.: Ocean acidification changes the structure of an Antarctic coastal protistan community, submitted.

35   Hauck, J. and Völker, C.: Rising atmospheric CO_2 leads to large impact of biology on Southern Ocean CO_2 uptake via changes of the Revelle factor, Geophys. Res. Lett., 42, 1459–1464, doi:10.1002/2015GL063070, 2015.

Hauck, J., Völker, C., Wolf-Gladrow, D. A., Laufkötter, C., Vogt, M., Aumont, O., Bopp, L., Buitenhuis, E. T., Doney, S. C., Dunne, J., Gruber, N., Hashioka, T., John, J., Quéré, C. L., Lima, I. D., Nakano, H., Séférian, R., and Totterdell, I.: On the Southern Ocean CO_2 uptake and

the role of the biological carbon pump in the 21st century, Global Biogeochem. Cycles, 29, 1451–1470, doi:10.1002/2015GB005140, 2015.

Hennon, G. M. M., Quay, P., Morales, R. L., Swanson, L. M., and Virginia Armbrust, E.: Acclimation conditions modify physiological response of the diatom *Thalassiosira pseudonana* to elevated CO_2 concentrations in a nitrate-limited chemostat, J. Phycol., 50, 243–253, doi:10.1111/jpy.12156, 2014.

Hennon, G. M. M., Ashworth, J., Groussman, R. D., Berthiaume, C., Morales, R. L., Baliga, N. S., Orellana, M. V., and Armbrust, E. V.: Diatom acclimation to elevated CO_2 via cAMP signalling and coordinated gene expression, Nat. Clim. Chang., 5, 761–765, doi:10.1038/nclimate2683, 2015.

Holding, J. M., Duarte, C. M., Sanz-Martín, M., Mesa, E., Arrieta, J. M., Chierici, M., Hendriks, I. E., García-Corral, L. S., Regaudie-de Gioux, A., Delgado, A., Reigstad, M., Wassmann, P., and Agustí, S.: Temperature dependence of CO_2-enhanced primary production in the European Arctic Ocean, Nat. Clim. Chang., 5, 1079–1082, doi:10.1038/nclimate2768, 2015.

Hong, H., Li, D., Lin, W., Li, W., and Shi, D.: Nitrogen nutritional condition affects the response of energy metabolism in diatoms to elevated carbon dioxide, Mar. Ecol. Prog. Ser., 567, 41–56, doi:10.3354/meps12033, 2017.

Honjo, S.: Particle export and the biological pump in the Southern Ocean, Antarct. Sci., 16, 501–516, doi:10.1017/S0954102004002287, 2004.

Hopkinson, B. M., Xu, Y., Shi, D., McGinn, P. J., and Morel, F. M. M.: The effect of CO_2 on the photosynthetic physiology of phytoplankton in the Gulf of Alaska, Limnol. Oceanogr., 55, 2011–2024, doi:10.4319/lo.2010.55.5.2011, 2010.

Hopkinson, B. M., Dupont, C. L., Allen, A. E., and Morel, F. M. M.: Efficiency of the CO_2-concentrating mechanism of diatoms, Proc. Natl. Acad. Sci., 108, 3830–3837, doi:10.1073/pnas.1018062108, 2011.

Hoppe, C. J. M., Hassler, C. S., Payne, C. D., Tortell, P. D., Rost, B., and Trimborn, S.: Iron Limitation Modulates Ocean Acidification Effects on Southern Ocean Phytoplankton Communities, PLoS One, 8, e79 890, doi:10.1371/journal.pone.0079890, 2013.

Hoppe, C. J. M., Holtz, L.-M., Trimborn, S., and Rost, B.: Ocean acidification decreases the light-use efficiency in an Antarctic diatom under dynamic but not constant light, New Phytol., 207, 159–171, doi:10.1111/nph.13334, 2015.

Hoppema, M., Fahrbach, E., Schröder, M., Wisotzki, A., and de Baar, H. J.: Winter-summer differences of carbon dioxide and oxygen in the Weddell Sea surface layer, Mar. Chem., 51, 177–192, doi:10.1016/0304-4203(95)00065-8, 1995.

IPCC: Climate Change 2013: The Physical Science Basis. Contribution of Working Group I to the Fifth Assessment Report of the Intergovernmental Panel on Climate Change, Cambridge University Press, Cambridge, United Kingdom and New York, NY, USA, doi:10.1017/CBO9781107415324, 2013.

Jeffrey, S. and Humphrey, G.: New spectrophotometric equations for determining chlorophylls a, b, c1 and c2 in higher plants, algae and natural phytoplankton, Biochem. und Physiol. der Pflanz., 167, 191–194, doi:10.1016/S0015-3796(17)30778-3, 1975.

Jeffrey, S. W. and Wright, S. W.: Qualitative and quantitative HPLC analysis of SCOR reference algal cultures, in: Phytoplankton Pigments in Oceanography: Guidelines to Modern Methods, edited by Jeffrey, S., Mantoura, R., and Wright, S., pp. 343–360, UNESCO, Paris, 1997.

Kähler, P. and Koeve, W.: Marine dissolved organic matter: Can its C:N ratio explain carbon overconsumption?, Deep. Res. Part I Oceanogr. Res. Pap., 48, 49–62, doi:10.1016/S0967-0637(00)00034-0, 2001.

Khatiwala, S., Primeau, F., and Hall, T.: Reconstruction of the history of anthropogenic CO_2 concentrations in the ocean, Nature, 462, 346–349, doi:10.1038/nature08526, 2009.

Kim, J.-M., Lee, K., Shin, K., Kang, J.-H., Lee, H.-W., Kim, M., Jang, P.-G., and Jang, M.-C.: The effect of seawater CO_2 concentration on growth of a natural phytoplankton assemblage in a controlled mesocosm experiment, Limnol. Oceanogr., 51, 1629–1636, doi:10.4319/lo.2006.51.4.1629, 2006.

King, A., Jenkins, B., Wallace, J., Liu, Y., Wikfors, G., Milke, L., and Meseck, S.: Effects of CO_2 on growth rate, C:N:P, and fatty acid

5   composition of seven marine phytoplankton species, Mar. Ecol. Prog. Ser., 537, 59–69, doi:10.3354/meps11458, 2015.

Kirchman, D. L.: Measuring Bacterial Biomass Production and Growth Rates from Leucine Incorporation in Natural Aquatic Environments, in: Methods in Microbiology, edited by Paul, J., vol. 30, chap. 12, pp. 227–237, Academic Press, St Petersburg, FL, doi:10.1016/S0580-9517(01)30047-8, 2001.

Kirchman, D. L.: Microbial ecology of the oceans, Wiley-Blackwell, Hoboken, N.J., 2 edn., 2008.

10   Legendre, L., Ackley, S. F., Dieckmann, G. S., Gulliksen, B., Horner, R., Hoshiai, T., Melnikov, I. A., Reeburgh, W. S., Spindler, M., and Sullivan, C. W.: Ecology of sea ice biota - 2. Global significance, Polar Biol., 12, 429–444, doi:10.1007/BF00243114, 1992.

Lewis, M. and Smith, J.: A small volume, short-incubation-time method for measurement of photosynthesis as a function of incident irradiance, Mar. Ecol. Prog. Ser., 13, 99–102, doi:10.3354/meps013099, 1983.

Li, F., Beardall, J., Collins, S., and Gao, K.: Decreased photosynthesis and growth with reduced respiration in the model diatom *Phaeodactylum tricornutum*

15   grown under elevated CO_2 over 1800 generations, Glob. Chang. Biol., 23, 127–137, doi:10.1111/gcb.13501, 2017a.

Li, W., Yang, Y., Li, Z., Xu, J., and Gao, K.: Effects of seawater acidification on the growth rates of the diatom *Thalassiosira (Conticribra) weissflogii* under different nutrient, light, and UV radiation regimes, J. Appl. Phycol., 29, 133–142, doi:10.1007/s10811-016-0944-y, 2017b.

Liu, N., Beardall, J., and Gao, K.: Elevated CO_2 and associated seawater chemistry do not benefit a model diatom grown with increased

20   availability of light, Aquat. Microb. Ecol., 79, 137–147, doi:10.3354/ame01820, 2017.

Longhurst, A. R.: Role of the marine biosphere in the global carbon cycle, Limnol. Oceanogr., 36, 1507–1526, doi:10.4319/lo.1991.36.8.1507, 1991.

Lueker, T. J., Dickson, A. G., and Keeling, C. D.: Ocean pCO_2 calculated from dissolved inorganic carbon, alkalinity, and equations for K_1 and K_2: validation based on laboratory measurements of CO_2 in gas and seawater at equilibrium, Mar. Chem., 70, 105–119,

25   doi:10.1016/S0304-4203(00)00022-0, 2000.

Mantoura, R. and Repeta, D.: Calibration methods for HPLC, in: Phytoplankton Pigments in Oceanography: Guidelines to Modern Methods, edited by Jeffrey, S., Mantoura, R., and Wright, S., pp. 407–428, UNESCO, Paris, 1997.

Marie, D., Simon, N., and Vaulot, D.: Phytoplankton cell counting by flow cytometry, in: Algal Culturing Techniques, edited by Anderson, R. A., chap. 17, pp. 253–267, Academic Press, San Diego, CA, USA, doi:10.1016/B978-012088426-1/50018-4, 2005.

30   McMinn, A., Müller, M. N., Martin, A., and Ryan, K. G.: The Response of Antarctic Sea Ice Algae to Changes in pH and CO2, PLoS One, 9, e86 984, doi:10.1371/journal.pone.0086984, 2014.

McNeil, B. I. and Matear, R. J.: Southern Ocean acidification: A tipping point at 450-ppm atmospheric CO_2, Proc. Natl. Acad. Sci., 105, 18 860–18 864, doi:10.1073/pnas.0806318105, 2008.

Mehrbach, C., Culberson, C. H., Hawley, J. E., and Pytkowicx, R. M.: Measurement of the Apparent Dissociation Constants of Carbonic

35   Acid in Seawater At Atmospheric Pressure, Limnol. Oceanogr., 18, 897–907, doi:10.4319/lo.1973.18.6.0897, 1973.

Meinshausen, M., Smith, S. J., Calvin, K., Daniel, J. S., Kainuma, M. L. T., Lamarque, J., Matsumoto, K., Montzka, S. A., Raper, S. C. B., Riahi, K., Thomson, A., Velders, G. J. M., and van Vuuren, D. P. P.: The RCP greenhouse gas concentrations and their extensions from 1765 to 2300, Clim. Change, 109, 213–241, doi:10.1007/s10584-011-0156-z, 2011.

Metzl, N., Tilbrook, B., and Poisson, A.: The annual $f\mathrm{CO_2}$ cycle and the air-sea $\mathrm{CO_2}$ flux in the sub-Antarctic Ocean, Tellus B, 51, 849–861, doi:10.1034/j.1600-0889.1999.t01-3-00008.x, 1999.

Moreau, S., Schloss, I., Mostajir, B., Demers, S., Almandoz, G., Ferrario, M., and Ferreyra, G.: Influence of microbial community composition and metabolism on air-sea $\Delta p\mathrm{CO_2}$ variation off the western Antarctic Peninsula, Mar. Ecol. Prog. Ser., 446, 45–59, doi:10.3354/meps09466, 2012.

Nelson, D. M., Smith, W. O. J., Gordon, L. I., and Huber, B. A.: Spring distributions of density, nutrients, and phytoplankton biomass in the ice edge zone of the Weddell-Scotia Sea, J. Geophys. Res. Ocean., 92, 7181, doi:10.1029/JC092iC07p07181, 1987.

Orr, J. C., Fabry, V. J., Aumont, O., Bopp, L., Doney, S. C., Feely, R. A., Gnanadesikan, A., Gruber, N., Ishida, A., Joos, F., Key, R. M., Lindsay, K., Maier-Reimer, E., Matear, R., Monfray, P., Mouchet, A., Najjar, R. G., Plattner, G.-K., Rodgers, K. B., Sabine, C. L., Sarmiento, J. L., Schlitzer, R., Slater, R. D., Totterdell, I. J., Weirig, M.-F., Yamanaka, Y., and Yool, A.: Anthropogenic ocean acidification over the twenty-first century and its impact on calcifying organisms, Nature, 437, 681–6, doi:10.1038/nature04095, 2005.

Pasquer, B., Mongin, M., Johnston, N., and Wright, S.: Distribution of particulate organic matter (POM) in the Southern Ocean during BROKE-West (30°E - 80°E), Deep Sea Res. Part II Top. Stud. Oceanogr., 57, 779–793, doi:10.1016/j.dsr2.2008.12.040, 2010.

Paul, C., Matthiessen, B., and Sommer, U.: Warming, but not enhanced $\mathrm{CO_2}$ concentration, quantitatively and qualitatively affects phytoplankton biomass, Mar. Ecol. Prog. Ser., 528, 39–51, doi:10.3354/meps11264, 2015.

Paulino, A. I., Egge, J. K., and Larsen, A.: Effects of increased atmospheric $\mathrm{CO_2}$ on small and intermediate sized osmotrophs during a nutrient induced phytoplankton bloom, Biogeosciences, 5, 739–748, doi:10.5194/bg-5-739-2008, 2008.

Pearce, I., Davidson, A., Bell, E., and Wright, S.: Seasonal changes in the concentration and metabolic activity of bacteria and viruses at an Antarctic coastal site, Aquat. Microb. Ecol., 47, 11–23, doi:10.3354/ame047011, 2007.

Pearce, I., Davidson, A. T., Thomson, P. G., Wright, S., and van den Enden, R.: Marine microbial ecology off East Antarctica (30 - 80°E): Rates of bacterial and phytoplankton growth and grazing by heterotrophic protists, Deep Sea Res. Part II Top. Stud. Oceanogr., 57, 849–862, doi:10.1016/j.dsr2.2008.04.039, 2010.

Perrin, R. A., Lu, P., and Marchant, H. J.: Seasonal variation in marine phytoplankton and ice algae at a shallow antarctic coastal site, Hydrobiologia, 146, 33–46, doi:10.1007/BF00007575, 1987.

Petrou, K., Kranz, S. A., Trimborn, S., Hassler, C. S., Ameijeiras, S. B., Sackett, O., Ralph, P. J., and Davidson, A. T.: Southern Ocean phytoplankton physiology in a changing climate, J. Plant Physiol., 203, 135–150, doi:10.1016/j.jplph.2016.05.004, 2016.

Piontek, J., Borchard, C., Sperling, M., Schulz, K. G., Riebesell, U., and Engel, A.: Response of bacterioplankton activity in an Arctic fjord system to elevated $p\mathrm{CO_2}$: results from a mesocosm perturbation study, Biogeosciences, 10, 297–314, doi:10.5194/bg-10-297-2013, 2013.

Platt, T., Gallegos, C. L., and Harrison, W. G.: Photoinibition of photosynthesis in natural assemblages of marine phytoplankton, J. Mar. Res., 38, 687–701, doi:citeulike-article-id:3354339, 1980.

Polimene, L., Sailley, S., Clark, D., Mitra, A., and Allen, J. I.: Biological or microbial carbon pump? The role of phytoplankton stoichiometry in ocean carbon sequestration, J. Plankton Res., 39, 180–186, doi:10.1093/plankt/fbw091, 2016.

R Core Team: R: A Language and Environment for Statistical Computing, R Foundation for Statistical Computing, Vienna, Austria, https://www.R-project.org/, 2016.

Raven, J. A.: Physiology of inorganic C acquisition and implications for resource use efficiency by marine phytoplankton: relation to increased $\mathrm{CO_2}$ and temperature, Plant, Cell Environ., 14, 779–794, doi:10.1111/j.1365-3040.1991.tb01442.x, 1991.

Raven, J. A. and Falkowski, P. G.: Oceanic sinks for atmospheric $\mathrm{CO_2}$, Plant, Cell Environ., 22, 741–755, doi:10.1046/j.1365-3040.1999.00419.x, 1999.

Raven, J. A., Caldeira, K., Elderfield, H., Hoegh-Guldberg, O., Liss, P., Riebesell, U., Shepherd, J., Turley, C., and Watson, A.: Ocean acidification due to increasing atmospheric carbon dioxide, Tech. Rep. June, The Royal Society, 2005.

Regaudie-de gioux, A., Lasternas, S., Agustí, S., Duarte, C. M., and Benitez, N. G.: Comparing marine primary production estimates through different methods and development of conversion equations, Front. Mar. Sci., 1, 1–14, doi:10.3389/fmars.2014.00019, 2014.

5   Riebesell, U.: Effects of CO_2 Enrichment on Marine Phytoplankton, J. Oceanogr., 60, 719–729, doi:10.1007/s10872-004-5764-z, 2004.

Riebesell, U., Schulz, K. G., Bellerby, R. G. J., Botros, M., Fritsche, P., Meyerhöfer, M., Neill, C., Nondal, G., Oschlies, A., Wohlers, J., and Zöllner, E.: Enhanced biological carbon consumption in a high CO_2 ocean, Nature, 450, 545–548, doi:10.1038/nature06267, 2007.

Riebesell, U., Gattuso, J.-P., Thingstad, T. F., and Middelburg, J. J.: Preface "Arctic ocean acidification: pelagic ecosystem and biogeochemical responses during a mesocosm study", Biogeosciences, 10, 5619–5626, doi:10.5194/bg-10-5619-2013, 2013.

10   Riley, G. A.: Phytoplankton of the North Central Sargasso Sea, 1950-521, Limnol. Oceanogr., 2, 252–270, doi:10.1002/lno.1957.2.3.0252, 1957.

Ritchie, R. J.: Consistent sets of spectrophotometric chlorophyll equations for acetone, methanol and ethanol solvents, Photosynth. Res., 89, 27–41, doi:10.1007/s11120-006-9065-9, 2006.

Roden, N. P., Shadwick, E. H., Tilbrook, B., and Trull, T. W.: Annual cycle of carbonate chemistry and decadal change in coastal Prydz Bay, East Antarctica, Mar. Chem., 155, 135–147, doi:10.1016/j.marchem.2013.06.006, 2013.

15   Rost, B., Riebesell, U., Burkhardt, S., and Sültemeyer, D.: Carbon acquisition of bloom-forming marine phytoplankton, Limnol. Oceanogr., 48, 55–67, doi:10.4319/lo.2003.48.1.0055, 2003.

Sabine, C. L., Feely, R. A., Gruber, N., Key, R. M., Lee, K., Bullister, J. L., Wanninkhof, R., Wong, C. S., Wallace, D. W. R., Tilbrook, B., Millero, F. J., Peng, T.-H., Kozyr, A., Ono, T., and Rios, A. F.: The Oceanic Sink for Anthropogenic CO_2, Science, 305, 367–371, doi:10.1126/science.1097403, 2004.

20

Satoh, A., Kurano, N., and Miyachi, S.: Inhibition of photosynthesis by intracellular carbonic anhydrase in microalgae under excess concentrations of CO_2, Photosynth. Res., 68, 215–224, doi:10.1023/A:1012980223847, 2001.

Schaum, C. E. and Collins, S.: Plasticity predicts evolution in a marine alga, Proc. R. Soc. B Biol. Sci., 281, 20141486–20141486, doi:10.1098/rspb.2014.1486, 2014.

25   Schaum, E., Rost, B., Millar, A. J., and Collins, S.: Variation in plastic responses of a globally distributed picoplankton species to ocean acidification, Nat. Clim. Chang., 3, 298–302, doi:10.1038/nclimate1774, 2012.

Schreiber, U.: Pulse-Amplitude-Modulation (PAM) Fluorometry and Saturation Pulse Method: An Overview, in: Chlorophyll a Fluorescence, edited by Papageorgiou, G. C. and Govindjee, pp. 279–319, Springer Netherlands, Dordrecht, doi:10.1007/978-1-4020-3218-9_11, 2004.

Schulz, K. G., Bellerby, R. G. J., Brussaard, C. P. D., Büdenbender, J., Czerny, J., Engel, A., Fischer, M., Koch-Klavsen, S., Krug, S. A.,
30   Lischka, S., Ludwig, A., Meyerhöfer, M., Nondal, G., Silyakova, A., Stuhr, A., and Riebesell, U.: Temporal biomass dynamics of an Arctic plankton bloom in response to increasing levels of atmospheric carbon dioxide, Biogeosciences, 10, 161–180, doi:10.5194/bg-10-161-2013, 2013.

Schulz, K. G., Bach, L. T., Bellerby, R. G. J., Bermúdez, R., Büdenbender, J., Boxhammer, T., Czerny, J., Engel, A., Ludwig, A., Meyerhöfer, M., Larsen, A., Paul, A. J., Sswat, M., and Riebesell, U.: Phytoplankton Blooms at Increasing Levels of Atmospheric Carbon
35   Dioxide: Experimental Evidence for Negative Effects on Prymnesiophytes and Positive on Small Picoeukaryotes, Front. Mar. Sci., 4, 64, doi:10.3389/fmars.2017.00064, 2017.

Shi, D., Xu, Y., and Morel, F. M. M.: Effects of the pH/pCO_2 control method on medium chemistry and phytoplankton growth, Biogeosciences, 6, 1199–1207, doi:10.5194/bg-6-1199-2009, 2009.

Shi, Q., Xiahou, W., and Wu, H.: Photosynthetic responses of the marine diatom *Thalassiosira pseudonana* to CO_2-induced seawater acidification, Hydrobiologia, 788, 361–369, doi:10.1007/s10750-016-3014-1, 2017.

Silsbe, G. M. and Malkin, S. Y.: phytotools: Phytoplankton Production Tools, https://CRAN.R-project.org/package=phytotools, r package version 1.0, 2015.

Simon, M. and Azam, F.: Protein content and protein synthesis rates of planktonic marine bacteria, Mar. Ecol. Prog. Ser., 51, 201–213, doi:10.3354/meps051201, 1989.

Smith, W. O. and Nelson, D. M.: Importance of Ice Edge Phytoplankton Production in the Southern Ocean, Bioscience, 36, 251–257, doi:10.2307/1310215, 1986.

Sobrino, C., Ward, M. L., and Neale, P. J.: Acclimation to elevated carbon dioxide and ultraviolet radiation in the diatom *Thalassiosira pseudonana*: Effects on growth, photosynthesis, and spectral sensitivity of photoinhibition, Limnol. Oceanogr., 53, 494–505, doi:10.4319/lo.2008.53.2.0494, 2008.

Sommer, U., Paul, C., and Moustaka-Gouni, M.: Warming and Ocean Acidification Effects on Phytoplankton—From Species Shifts to Size Shifts within Species in a Mesocosm Experiment, PLoS One, 10, e0125 239, doi:10.1371/journal.pone.0125239, 2015.

Sperling, M., Piontek, J., Gerdts, G., Wichels, A., Schunck, H., Roy, A.-S., La Roche, J., Gilbert, J., Nissimov, J. I., Bittner, L., Romac, S., Riebesell, U., and Engel, A.: Effect of elevated CO_2 on the dynamics of particle-attached and free-living bacterioplankton communities in an Arctic fjord, Biogeosciences, 10, 181–191, doi:10.5194/bg-10-181-2013, 2013.

Spilling, K., Paul, A. J., Virkkala, N., Hastings, T., Lischka, S., Stuhr, A., Bermúdez, R., Czerny, J., Boxhammer, T., Schulz, K. G., Ludwig, A., and Riebesell, U.: Ocean acidification decreases plankton respiration: evidence from a mesocosm experiment, Biogeosciences, 13, 4707–4719, doi:10.5194/bg-13-4707-2016, 2016.

Steemann Nielsen, E.: The Use of Radio-active Carbon (C^{14}) for Measuring Organic Production in the Sea, ICES J. Mar. Sci., 18, 117–140, doi:10.1093/icesjms/18.2.117, 1952.

Takahashi, T., Sutherland, S. C., Wanninkhof, R., Sweeney, C., Feely, R. A., Chipman, D. W., Hales, B., Friederich, G., Chavez, F., Sabine, C., Watson, A., Bakker, D. C., Schuster, U., Metzl, N., Yoshikawa-Inoue, H., Ishii, M., Midorikawa, T., Nojiri, Y., Körtzinger, A., Steinhoff, T., Hoppema, M., Olafsson, J., Arnarson, T. S., Tilbrook, B., Johannessen, T., Olsen, A., Bellerby, R., Wong, C., Delille, B., Bates, N., and de Baar, H. J.: Climatological mean and decadal change in surface ocean pCO_2, and net sea–air CO_2 flux over the global oceans, Deep Sea Res. Part II Top. Stud. Oceanogr., 56, 554–577, doi:10.1016/j.dsr2.2008.12.009, 2009.

Takahashi, T., Sweeney, C., Hales, B., Chipman, D., Newberger, T., Goddard, J., Iannuzzi, R., and Sutherland, S.: The Changing Carbon Cycle in the Southern Ocean, Oceanography, 25, 26–37, doi:10.5670/oceanog.2012.71, 2012.

Tanaka, T., Alliouane, S., Bellerby, R. G. B., Czerny, J., de Kluijver, A., Riebesell, U., Schulz, K. G., Silyakova, A., and Gattuso, J.-P.: Effect of increased pCO_2 on the planktonic metabolic balance during a mesocosm experiment in an Arctic fjord, Biogeosciences, 10, 315–325, doi:10.5194/bg-10-315-2013, 2013.

Taylor, A. R., Brownlee, C., and Wheeler, G. L.: Proton channels in algae: reasons to be excited, Trends Plant Sci., 17, 675–684, doi:10.1016/j.tplants.2012.06.009, 2012.

Tew, K. S., Kao, Y.-C., Ko, F.-C., Kuo, J., Meng, P.-J., Liu, P.-J., and Glover, D. C.: Effects of elevated CO2 and temperature on the growth, elemental composition, and cell size of two marine diatoms: potential implications of global climate change, Hydrobiologia, 741, 79–87, doi:10.1007/s10750-014-1856-y, 2014.

Thomson, P., Davidson, A., and Maher, L.: Increasing CO_2 changes community composition of pico- and nano-sized protists and prokaryotes at a coastal Antarctic site, Mar. Ecol. Prog. Ser., 554, 51–69, doi:10.3354/meps11803, 2016.

Torstensson, A., Hedblom, M., Mattsdotter Björk, M., Chierici, M., and Wulff, A.: Long-term acclimation to elevated pCO_2 alters carbon metabolism and reduces growth in the Antarctic diatom *Nitzschia lecointei*, Proc. R. Soc. B Biol. Sci., 282, 20151513, doi:10.1098/rspb.2015.1513, 2015.

Tortell, P. D. and Morel, F. M. M.: Sources of inorganic carbon for phytoplankton in the eastern Subtropical and Equatorial Pacific Ocean, Limnol. Oceanogr., 47, 1012–1022, doi:10.4319/lo.2002.47.4.1012, 2002.

Tortell, P. D., Rau, G. H., and Morel, F. M. M.: Inorganic carbon acquisition in coastal Pacific phytoplankton communities, Limnol. Oceanogr., 45, 1485–1500, doi:10.4319/lo.2000.45.7.1485, 2000.

Tortell, P. D., Payne, C., Gueguen, C., Strzepek, R. F., Boyd, P. W., and Rost, B.: Inorganic carbon uptake by Southern Ocean phytoplankton, Limnol. Oceanogr., 53, 1266–1278, doi:10.4319/lo.2008.53.4.1266, 2008a.

Tortell, P. D., Payne, C. D., Li, Y., Trimborn, S., Rost, B., Smith, W. O. J., Riesselman, C., Dunbar, R. B., Sedwick, P., and DiTullio, G. R.: CO_2 sensitivity of Southern Ocean phytoplankton, Geophys. Res. Lett., 35, L04605, doi:10.1029/2007GL032583, 2008b.

Tortell, P. D., Trimborn, S., Li, Y., Rost, B., and Payne, C. D.: Inorganic carbon utilization by Ross Sea phytoplankton across natural and experimental CO_2 gradients, J. Phycol., 46, 433–443, doi:10.1111/j.1529-8817.2010.00839.x, 2010.

Tortell, P. D., Asher, E. C., Ducklow, H. W., Goldman, J. A. L., Dacey, J. W. H., Grzymski, J. J., Young, J. N., Kranz, S. A., Bernard, K. S., and Morel, F. M. M.: Metabolic balance of coastal Antarctic waters revealed by autonomous pCO_2 and ΔO_2/Ar measurements, Geophys. Res. Lett., 41, 6803–6810, doi:10.1002/2014GL061266, 2014.

Trimborn, S., Brenneis, T., Sweet, E., and Rost, B.: Sensitivity of Antarctic phytoplankton species to ocean acidification: Growth, carbon acquisition, and species interaction, Limnol. Oceanogr., 58, 997–1007, doi:10.4319/lo.2013.58.3.0997, 2013.

Trimborn, S., Thoms, S., Petrou, K., Kranz, S. A., and Rost, B.: Photophysiological responses of Southern Ocean phytoplankton to changes in CO_2 concentrations: Short-term versus acclimation effects, J. Exp. Mar. Bio. Ecol., 451, 44–54, doi:10.1016/j.jembe.2013.11.001, 2014.

van de Waal, D. B., Verschoor, A. M., Verspagen, J. M., van Donk, E., and Huisman, J.: Climate-driven changes in the ecological stoichiometry of aquatic ecosystems, Front. Ecol. Environ., 8, 145–152, doi:10.1890/080178, 2010.

Wang, Y., Zhang, R., Zheng, Q., Deng, Y., Van Nostrand, J. D., Zhou, J., and Jiao, N.: Bacterioplankton community resilience to ocean acidification: evidence from microbial network analysis, ICES J. Mar. Sci. J. du Cons., 73, 865–875, doi:10.1093/icesjms/fsv187, 2016.

Westwood, K., Thomson, P., van den Enden, R., Maher, L., Wright, S., and Davidson, A.: Ocean acidification impacts primary and bacterial production in Antarctic coastal waters during austral summer, submitted.

Westwood, K. J., Brian Griffiths, F., Meiners, K. M., and Williams, G. D.: Primary productivity off the Antarctic coast from 30°–80°E; BROKE-West survey, 2006, Deep Sea Res. Part II Top. Stud. Oceanogr., 57, 794–814, doi:10.1016/j.dsr2.2008.08.020, 2010.

Wright, S. W., van den Enden, R. L., Pearce, I., Davidson, A. T., Scott, F. J., and Westwood, K. J.: Phytoplankton community structure and stocks in the Southern Ocean (30-80°E) determined by CHEMTAX analysis of HPLC pigment signatures, Deep Sea Res. Part II Top. Stud. Oceanogr., 57, 758–778, doi:10.1016/j.dsr2.2009.06.015, 2010.

Wu, Y., Gao, K., and Riebesell, U.: CO_2-induced seawater acidification affects physiological performance of the marine diatom *Phaeodactylum tricornutum*, Biogeosciences, 7, 2915–2923, doi:10.5194/bg-7-2915-2010, 2010.

Young, J., Kranz, S., Goldman, J., Tortell, P., and Morel, F.: Antarctic phytoplankton down-regulate their carbon-concentrating mechanisms under high CO_2 with no change in growth rates, Mar. Ecol. Prog. Ser., 532, 13–28, doi:10.3354/meps11336, 2015.

Zheng, Y., Giordano, M., and Gao, K.: Photochemical responses of the diatom *Skeletonema costatum* grown under elevated CO_2 concentrations to short-term changes in pH, Aquat. Biol., 23, 109–118, doi:10.3354/ab00619, 2015.

Figure 1. Minicosm tanks filled with seawater in temperature controlled shipping container.
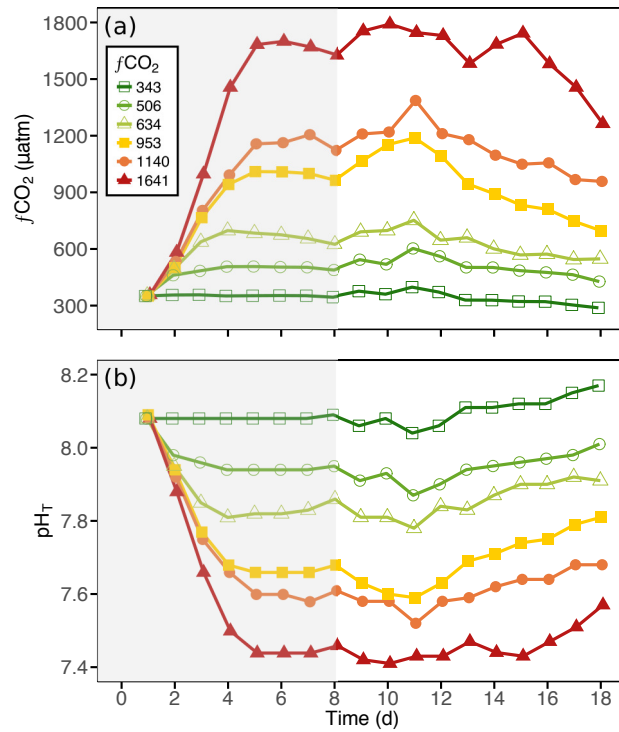
Figure 2. (a) $f\mathrm{CO_2}$ and (b) pH_T conditions within each of the minicosm treatments over time. Grey shading indicates $\mathrm{CO_2}$ and light acclimation period.
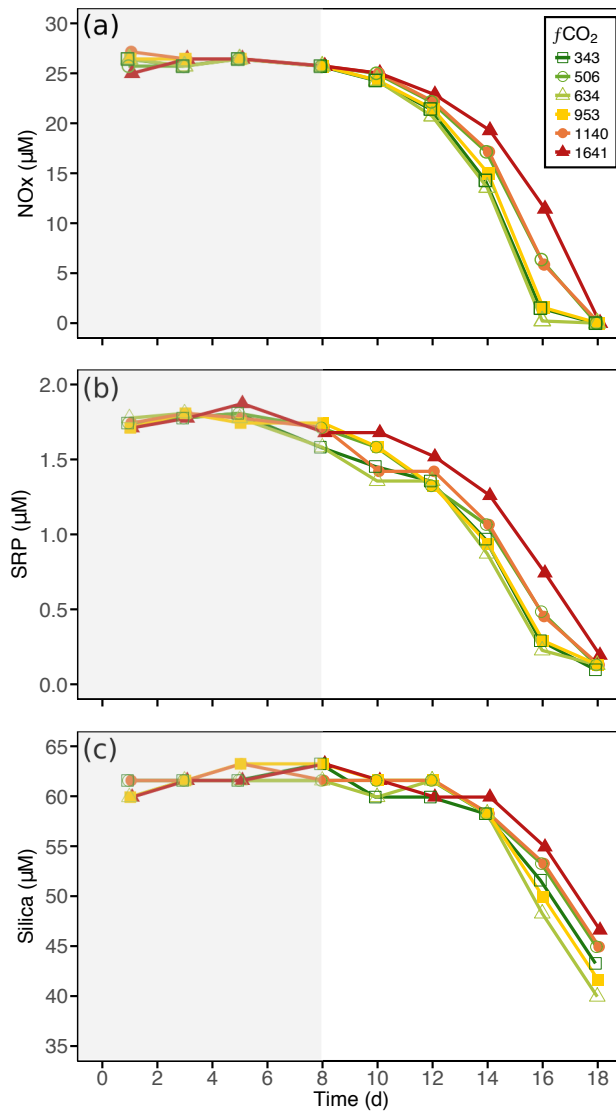
Figure 3. Nutrient draw-down within each of the minicosm treatments over time. (a) Nitrate + nitrite (NOx), (b) soluble reactive phosphorus (SRP), and (c) molybdate reactive silica (Silica). Grey shading indicates CO_2 and light acclimation period.
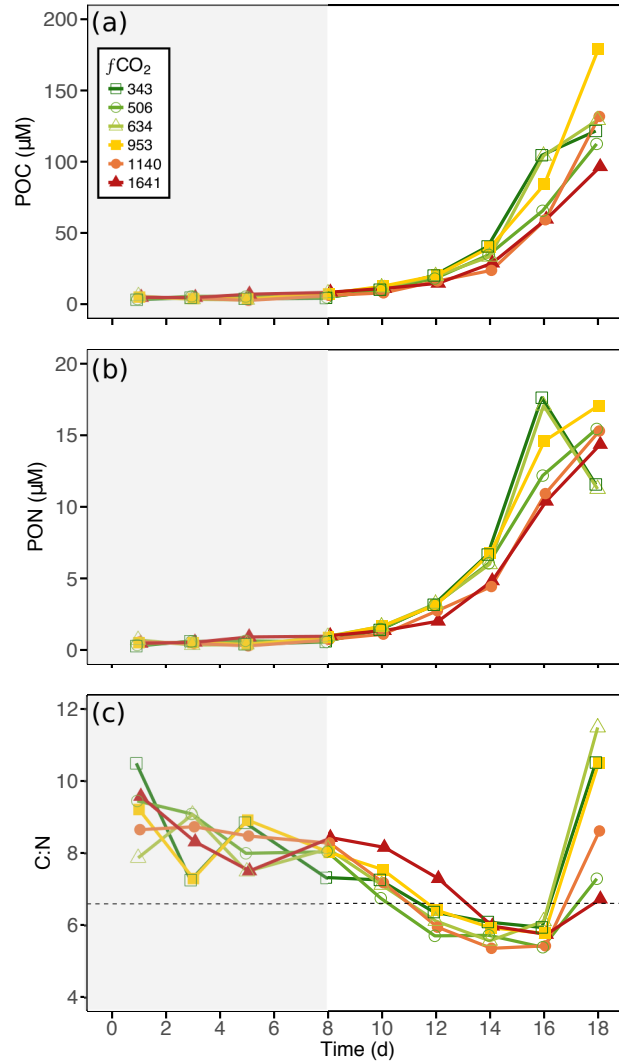
Figure 4. Particulate organic matter concentration and C:N ratio of each of the minicosm treatments over time. (a) Particulate organic carbon (POC), (b) particulate organic nitrogen (PON), and (c) carbon:nitrogen (C:N) ratio. Dashed line indicates C:N Redfield Ratio of 6.6. Grey shading indicates CO_2 and light acclimation period.
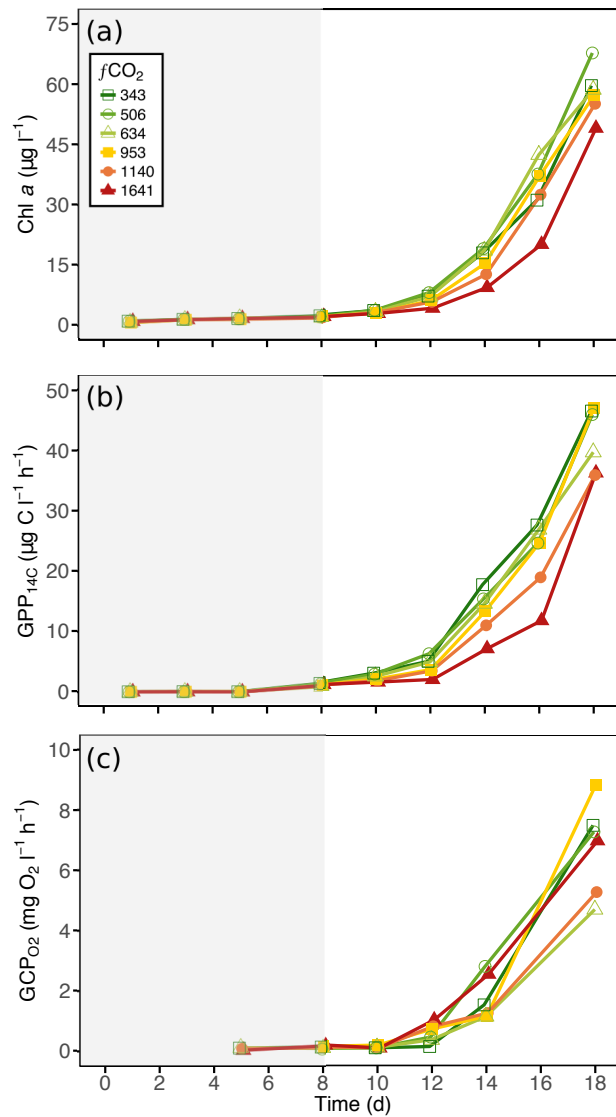
Figure 5. Phytoplankton biomass accumulation and community primary production in each of the minicosm treatments over time. (a) Chlorophyll *a* (Chl *a*) concentration, (b) ^{14}C-derived gross primary production (GPP_{14C}), and (c) O_2-derived gross community productivity (GCP_{O_2}). Error bars display one standard deviation of pseudoreplicate samples. Grey shading indicates CO_2 and light acclimation period.
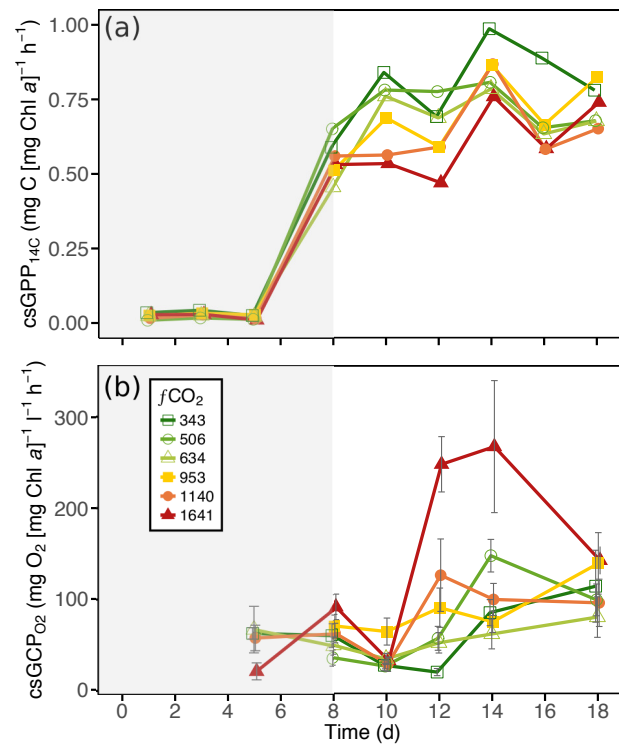
Figure 6. (a) ^{14}C-derived Chl *a*-specific primary productivity ($csGPP_{14C}$) and (b) O_2-derived Chl *a*-specific community productivity ($csGCP_{O_2}$) within each of the minicosm treatments over time. Grey shading indicates CO_2 and light acclimation period.
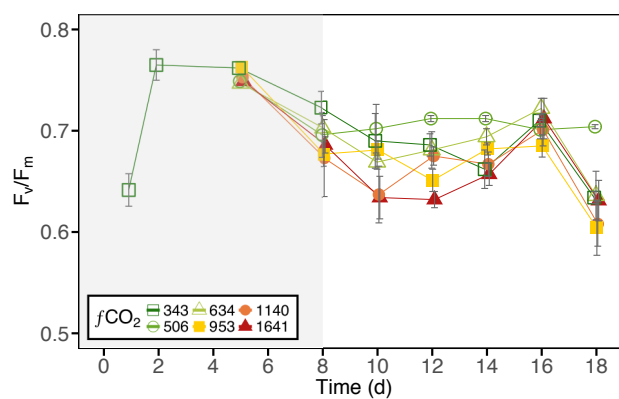
Figure 7. Maximum quantum yield of PSII (F_v/F_m) in each of the minicosm treatments over time. Error bars display one standard deviation of pseudoreplicate samples. Grey shading indicates CO_2 and light acclimation period.
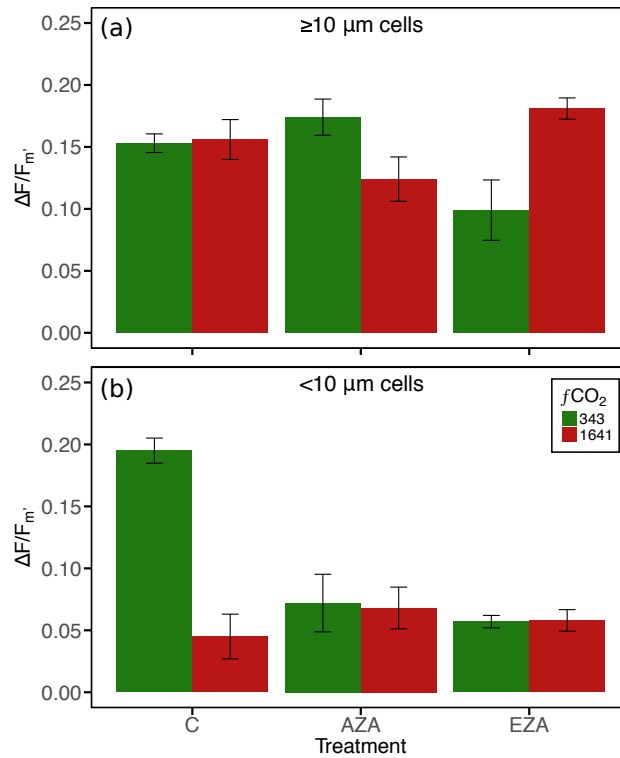
Figure 8. Effective quantum yield of PSII ($\Delta F/F_{m'}$) of (a) large ($\geq 10\,\mu m$) and (b) small ($<10\,\mu m$) phytoplankton in the control (343 µatm) and high (1641 µatm) CO_2 treatments treated with carbonic anhydrase (CA) inhibitors. A decline in $\Delta F/F_{m'}$ with application of inhibitor indicates CCM activity. C: control, no CA inhibitor, AZA: acetazolamide, blocks extracellular carbonic anhydrase, EZA: ethoxzolamide, blocks intracellular and extracellular carbonic anhydrase. Error bars display one standard deviation of pseudoreplicate samples.
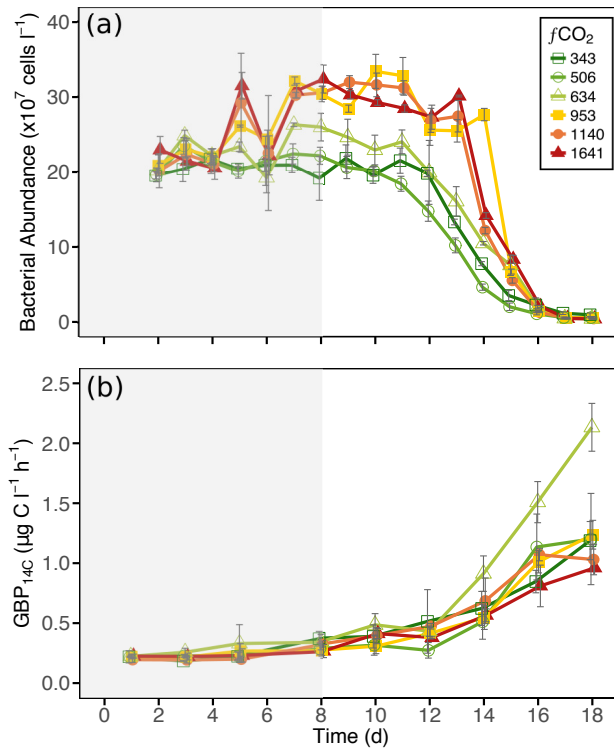
Figure 9. Bacterial abundance and community production in each of the minicosm treatments over time. (a) Bacterial cell abundance and (b) ^{14}C-derived gross bacterial production (GBP$_{14C}$). Error bars display one standard deviation of pseudoreplicate samples. Grey shading indicates CO_2 and light acclimation period.
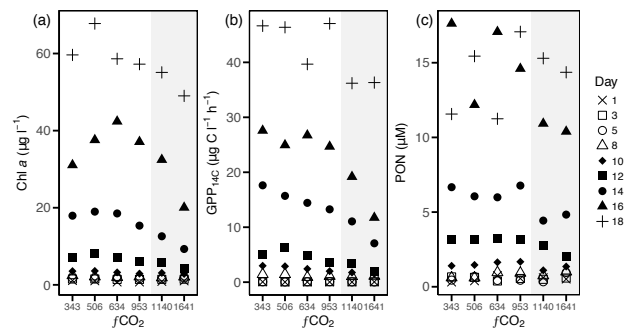
Figure 10. Fig. 10. Temporal trends of Chl *a*, ^{14}C-derived gross primary production (GPP$_{14C}$), and particulate organic nitrogen (PON) against CO_2 treatment. Grey shading indicates CO_2 treatments ≥ 1140 µatm.

Table 1. Definitions, measurements and calculations for productivity data

Name	Definition	Units	Measurements and calculations
Primary Productivity			
Carbon incorporation	Total ^{14}C-sodium bicarbonate incorporation	mg C (mg Chl a)$^{-1}$ l^{-1} h^{-1}	Equation from Steemann Nielsen (1952) $= \dfrac{(DPM_s - DPM_{T_0})}{DPM_{100\%}} \times DIC \times 1.05$ / time / Chl a
α	Maximum photosynthetic efficiency	mg C (mg Chl a)$^{-1}$ (μmol photons m^{-2} s^{-1})$^{-1}$ h^{-1}	Modelled from PE curve of 21 light intensities 0 - 1411 μmol photons m^{-2} s^{-1}
β	Photoinhibition rate	mg C (mg Chl a)$^{-1}$ (μmol photons m^{-2} s^{-1})$^{-1}$ h^{-1}	Modelled from PE curve of 21 light intensities 0 - 1411 μmol photons m^{-2} s^{-1}
P_{max}	Maximum photosynthetic rate	mg C (mg Chl a)$^{-1}$ l^{-1} h^{-1}	Equation from Platt et al. (1980) $= P_s \times \dfrac{\alpha}{(\alpha + \beta)} \times \dfrac{\beta}{(\alpha + \beta)}^{\frac{\beta}{\alpha}}$
E_k	Saturating irradiance	μmol photons m^{-2} s^{-1}	Equation from Platt et al. (1980) $= \dfrac{P_{max}}{\alpha}$
$\bar{I}$	Average irradiance received by phytoplankton cells	μmol photons m^{-2} s^{-1}	Equation from Riley (1957) $= \bar{I}_o(1 - e^{(-K_d \times Z_m)}) / (K_d \times Z_m)$
csGPP$_{14C}$	^{14}C Chl a-specific primary productivity	mg C (mg Chl a)$^{-1}$ h^{-1}	Equation from Platt et al. (1980) $= P_s \times e^{\frac{-\alpha I}{P_s}} \times e^{\frac{-\beta I}{P_s}}$
GPP$_{14C}$	^{14}C gross primary production	μg C l^{-1} h^{-1}	$= $ csGPP$_{14C} \times$ Chl a
csGCP$_{O_2}$	O$_2$ Chl a-specific gross community productivity	mg O$_2$ (mg Chl a)$^{-1}$ h^{-1}	$= $ NCP$_{O_2}$ + Resp$_{O_2}$ / Chl a
GCP$_{O_2}$	O$_2$ gross community production	mg O$_2$ l^{-1} h^{-1}	$= $ csGCP$_{O_2} \times$ Chl a
Photophysiology			
F$_v$/F$_m$	Maximum quantum yield of PSII	(arbitrary units)	$= \dfrac{F_m - F_O}{F_m}$
ΔF/F$_{m'}$	Effective quantum yield of PSII	(arbitrary units)	$= \dfrac{(F_{m'} - F)}{F_{m'}}$
rETR	Relative electron transport rate	(arbitrary units)	$= \dfrac{\Delta F_v}{F_{m'}} \times I_a$
NPQ	Non-photochemical quenching	(arbitrary units)	$= \dfrac{(F_m - F_{m'})}{F_{m'}}$
Bacterial Productivity			
nmol Leucine$_{inc}$	Moles of exogenous ^{14}C-Leucine incorporated	nmol l^{-1} h^{-1}	Equation from Kirchman (2001) $= (DPM_s - DPM_{t_0})$ / time / 2.22 $\times 10^6$ $\times$ SA (nmol μCi^{-1}) / sample vol (l)
GBP$_{14C}$	^{14}C gross bacterial production	μg C l^{-1} h^{-1}	Equation from Simon and Azam (1989) $= $ (nmol Leucine$_{inc}$ / 10^3) $\times$ 131.2 / 0.073 $\times$ 0.86 $\times$ 2
csBP$_{14C}$	^{14}C cell-specific bacterial productivity	fg C cell^{-1} l^{-1} h^{-1}	$= $ GBP$_{14C}$ / cells l^{-1}

P$_s$: maximum photosynthetic output with no photoinhibition, from Platt et al. (1980), DPM$_s$: sample DPM, SA: specific activity of ^{14}C-Leucine isotope

All other abbreviations defined in Methods Section

40